IMAGING OF SPORTS INJURIES OF THE ANKLE AND FOOT

DOUGLAS K. SMITH, MD

The foot and ankle are frequently injured during sporting events. In many cases, the diagnosis is apparent based on the history, physical examination, and plain radiographs. In other cases, the presentation may be confusing or nonspecific. In these cases, special imaging modalities may be useful to determine or confirm the diagnosis. This article will show examples of sports injuries for which special-imaging modalities may be particularly useful in determining the correct diagnosis, such as ligament and tendon injuries, normal variants, tarsal tunnel syndrome, occult fractures, and stress fractures.
KEY WORDS: fractures, ligaments, tendons

The foot and ankle are frequently injured during sporting events and may produce considerable disability in many athletes. Injuries of the foot and ankle may be acute or chronic problems. Cass and Morrey[1] reported that acute foot and ankle injuries accounted for 10% of emergency room visits. Garrick and Requa[2] reported that foot and ankle injuries represented over 25% of the 16,00 athletic injuries in their series. In many cases, an accurate diagnosis can be made using the history, physical examination, and plain radiographs; special-imaging modalities are not required to make or confirm the diagnosis. In many other cases, the diagnosis may not be as apparent. In these cases, special imaging may be useful in determining the correct diagnosis. This report will show some examples of how special-imaging modalities can be used to diagnose various clinical entities of the foot and ankle. The examples will be considered according to the anatomic structure that is effected (ie, ligaments, tendons, etc).

LIGAMENTS

Ligamentous structures are important for maintaining stability in the hindfoot and are frequently injured in sporting events. The anterior and posterior tibial and fibular ligaments (ATiFL and PTiFL) help to maintain the stability of the distal tibial and fibular syndesmosis and are transversely oriented at a level just above the tibiotalar joint (Fig 1).[3] At this level, the fibula has an oval shape with a convex posterior surface (Fig 1). The convex shape of the fibula distinguishes the PTiFL from the

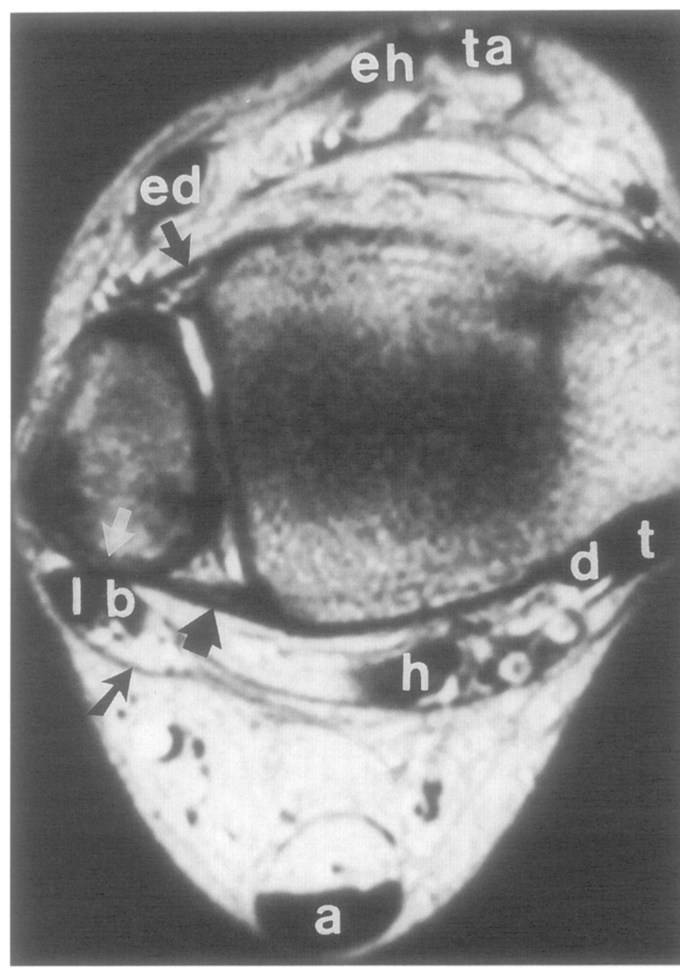

Fig 1. Axial T1-weighted MR image at level of distal tibial and fibular joint shows anterior (small straight arrow) and posterior (large straight arrow) tibiofibular ligaments. Peroneus longus (l) and peroneus brevis (b) tendons stabilized by superior peroneal retinaculum (oblique arrow) arising from the lateral malleolus and attaching to the calcaneus. Convex posterior border (white arrow) of lateral malleolus; ta, tibialis anterior tendon; eh, extensor hallucis longus tendon; ed, extensor digitorum longus tendon; t, tibialis posterior tendon; d, flexor digitorum longus tendon; h, flexor hallucis longus tendon; a, Achilles tendon.

From the Department of Radiology, Wilford Hall, USAF Medical Center, Lackland AFB, TX.
The views expressed in this article are those of the author and do not reflect the official policy of the Department of Defense or other departments of the US Government.
Address correspondence to Douglas K. Smith, Maj USAF MC, WHMC/PSRD, 220 Bergquist Dr, Ste 1, Lackland AFB, TX 78236-5300.

1060-1872/95/0301-0006$05.00/0

similarly oriented posterior talofibular ligament that is located at a lower level (Fig 2A).

There are three lateral collateral ligaments: the anterior and posterior talofibular ligaments (ATFL and PTFL) and the calcaneofibular ligament. The ATFL and PTFL are best seen in axial magnetic resonance (MR) images at the level of the posterior concavity of the fibula (Fig 2A). The ATFL is the most frequently injured ligament and the calcaneofibular ligament is the second most frequently injured lateral ligament (Fig 2B).

Some patients develop a focal soft-tissue mass and focal pain in the interval between the anterior tibia and fibula after a severe ankle sprain.[4] The term "meniscoid syndrome" has been coined to describe the hyalinized synovial tissue that is frequently found in the location of the mass. MR imaging of meniscoid syndrome shows low signal (dark) tissue in the interval between the anterior tibia and fibula (Fig 3).[4]

The PTFL attaches to the posterior process of the talus and may be avulsed during an ankle inversion injury. The PTFL is frequently seen using MR images in the coronal plane but can be misinterpreted as an osteochondral body using sagittal images (Fig 4). If the PTFL is followed on contiguous images it will not be mistaken for an osteochondral body. The os trigonum is an accessory ossification center of the posterior process of the talus and can be distinguished from a posterior process avulsion fracture by the absence of marrow or soft-tissue edema. An os trigonum has an undulating synostosis compared with a straight line fracture (Fig 5).

The medial collateral or deltoid ligament is composed of superficial (tibiocalcaneal) and deep (tibiotalar) fibers (Fig 6).[5-9] The deltoid ligament complex is composed of a group of fibers sharing the origin from the medial malleolus and arranged into superficial and deep layers.[8,10] The superficial fibers arise from the anterior colliculus: the tibiocalcaneal, tibiospring, and tibionavicular ligaments.[8,10] The deep layer is composed of the anterior and posterior tibiotalar ligaments.[8,10] The various components of the deltoid ligament complex (except the anterior tibiotalar ligament) can be consistently seen using multiplanar reconstructions of three-dimensional transform gradient-echo MR images.[8] In a series of 26 patients with medial ligamentous injuries, Klein et al[8] found tears of the tibionavicular ligament in 69%, the tibiocalcaneal ligament in 65%, tibiospring ligament in 35%, and the posterior tibiotalar ligament in 15%. The posterior tibiotalar and tibiocalcaneal ligaments are most easily seen using conventional coronal plane imaging (Fig 6). When these structures are torn, the more anteriorly lo-

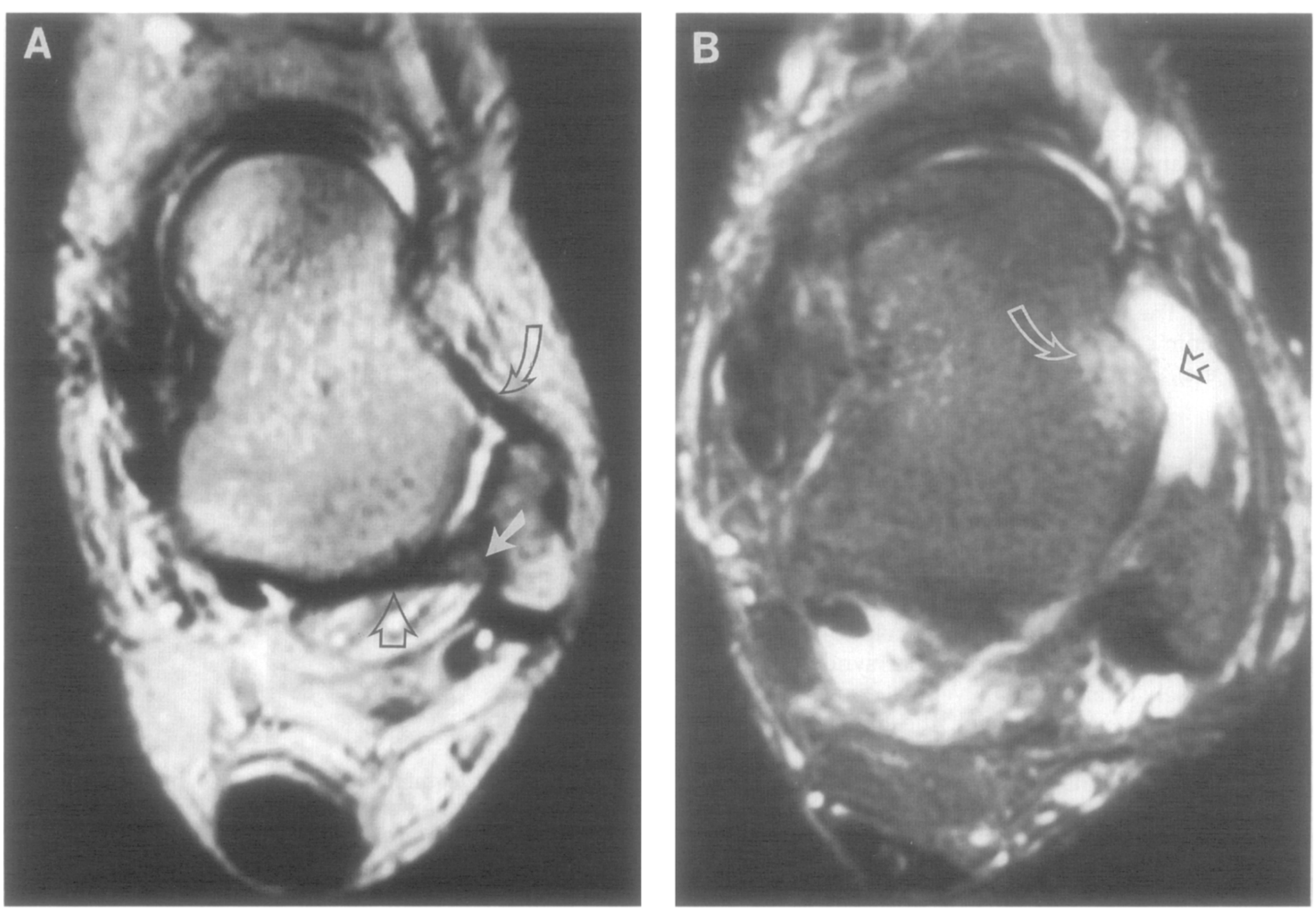

Fig 2. (A) Axial fast-spin echo, T2-weighted MR image through posterior concavity (white arrow) of fibula at level of talar body shows intact anterior (curved open arrow) and posterior (straight open arrow) talofibular ligaments. Notice that the fluid in ankle joint abuts posterior surface anterior talofibular ligament. (B) Axial fast-spin echo, T2-weighted MR image with fat suppression shows disrupted anterior talofibular ligament (ATFL, open arrow) with marrow edema (curved open arrow: bright signal of lateral talus).

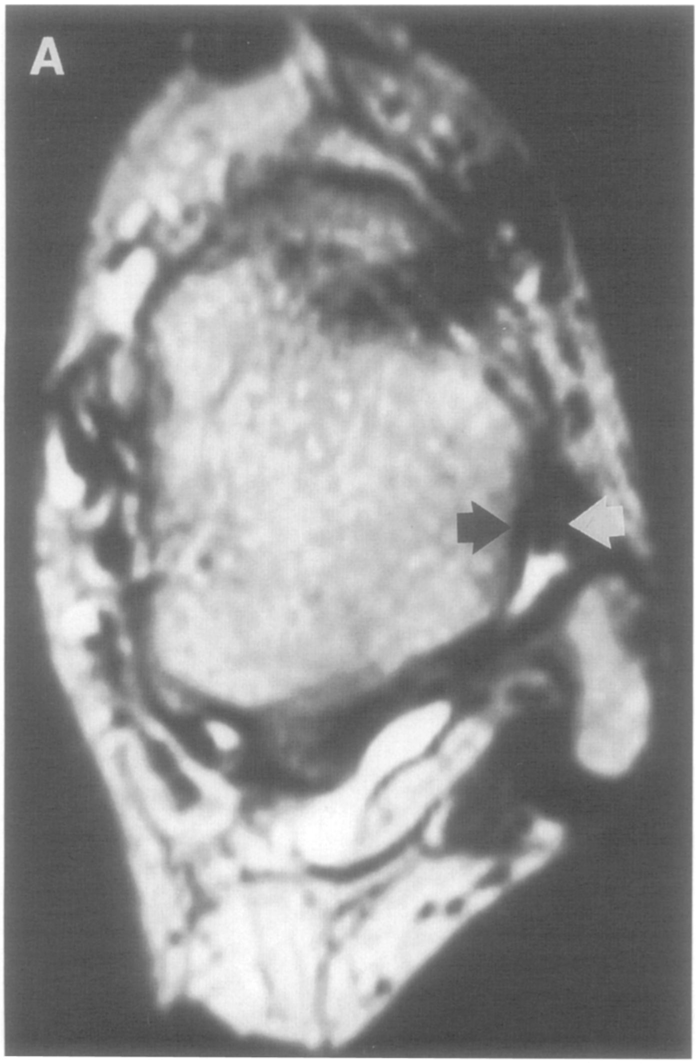

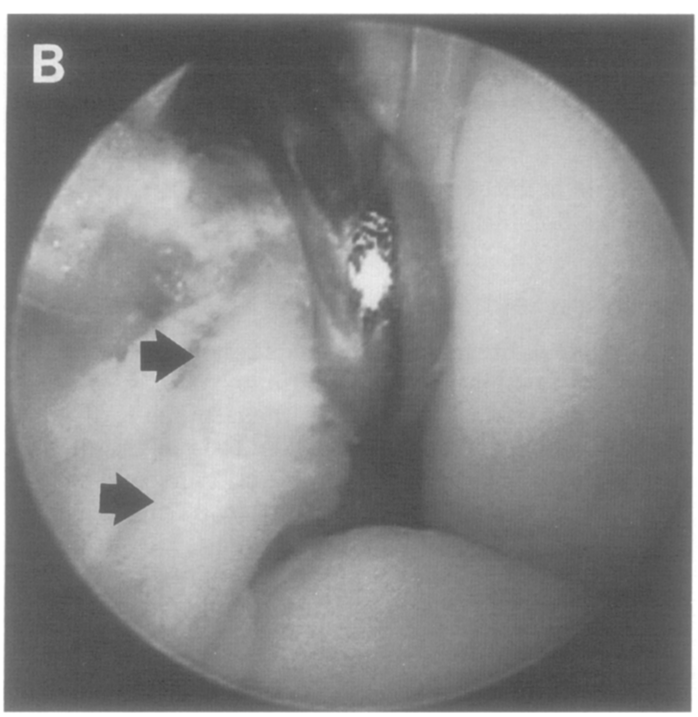

Fig 3. (A) Axial T2-weighted image of patient with meniscoid syndrome: low signal soft-tissue mass located in margin between talus and fibula (between black and white arrows). (B) Arthroscopic view of same patient with probe around hyalinized synovial tissue (meniscoid tissue) seen by MR imaging. (Courtesy of Jim Gilley, MD, San Antonio, TX.)

cated ligaments (tibionavicular and anterior tibiotalar) were invariably torn. The deltoid ligaments are torn during an ankle eversion injury and are less commonly torn than fibers of the lateral collateral ligaments.

TENDONS

Eleven tendons normally cross the ankle joint: (1) posterior group: Achilles and plantaris tendons; (2) extensor group: tibialis anterior, extensor digitorum longus, extensor hallucis longus, and peroneus tertius; (3) flexor group: tibialis posterior, flexor digitorum longus, and flexor hallucis longus; and (4) peroneal group: peroneus longus and peroneus brevis (Fig 7). Each of these structures can be effected by sports injuries and will be discussed separately.

Achilles Tendon

Achilles tendon injuries may be chronic (tendonitis) or acute (rupture) injuries. Chronic Achilles tendonitis effects up to 11% of runners and is usually related to improper shoe wear or running uphill.[11] Achilles tendonitis is also common in racket sports and usually effects men between 30 and 50 years old.[12] Repeated stresses produce internal degeneration of the tendon with accumulation of granulation tissue approximately 3.75 cm above the insertion into the os calcis.[13] Acute Achilles tendon ruptures are common injuries and may affect both poorly trained "weekend jocks" as well as well-trained athletes.[14] Almost 60% of acute ruptures occur during sporting events and usually result from rapid dorsiflexion (stretching of the tendon) during jumping or running events.[15]

The Achilles tendon is the largest tendon in the body.[3] It originates at the confluence of the gastrocnemius and soleus muscles and has broad attachment along the posterior and plantar surfaces of the calcaneus.[3] The Achilles tendon is approximately 15 cm in length and tapers into a curved ribbon shape with a posterior convexity at a point several centimeters its insertion into the calcaneus.[3] Most injuries affect the tendon 2 to 6 cm proximal to the calcaneal insertion where the tendon is thinnest and the vascularity is tenuous.[3,16]

The normal Achilles tendon is black on all MR-imaging sequences and tapers smoothly from its origin in the midcalf to its insertion into the calcaneus (Fig 8).[6,14,17-19] MR imaging in the sagittal and axial planes are most useful for evaluating the Achilles tendon.[14] The plantaris tendon may appear as a tubular structure along the anteromedial margin of the Achilles tendon.[3] Chronic Achilles tendonitis or tendinosis may be recognized as a nodular or fusiform enlargement of the tendon located several centimeters above the calcaneal insertion (Fig 9).[20] MR images of chronic Achilles tendonitis using a short echo time (TE) (T1-weighted and proton-density–weighted images) will show patchy, intermediate (gray) signal within a enlarged tendon (Fig 9).[20] There may be evidence of subcutaneous edema (bright on T2 and dark on T1) or fibrosis (low signal on both sequences) associated with chronic Achilles tendonitis (Fig 9).

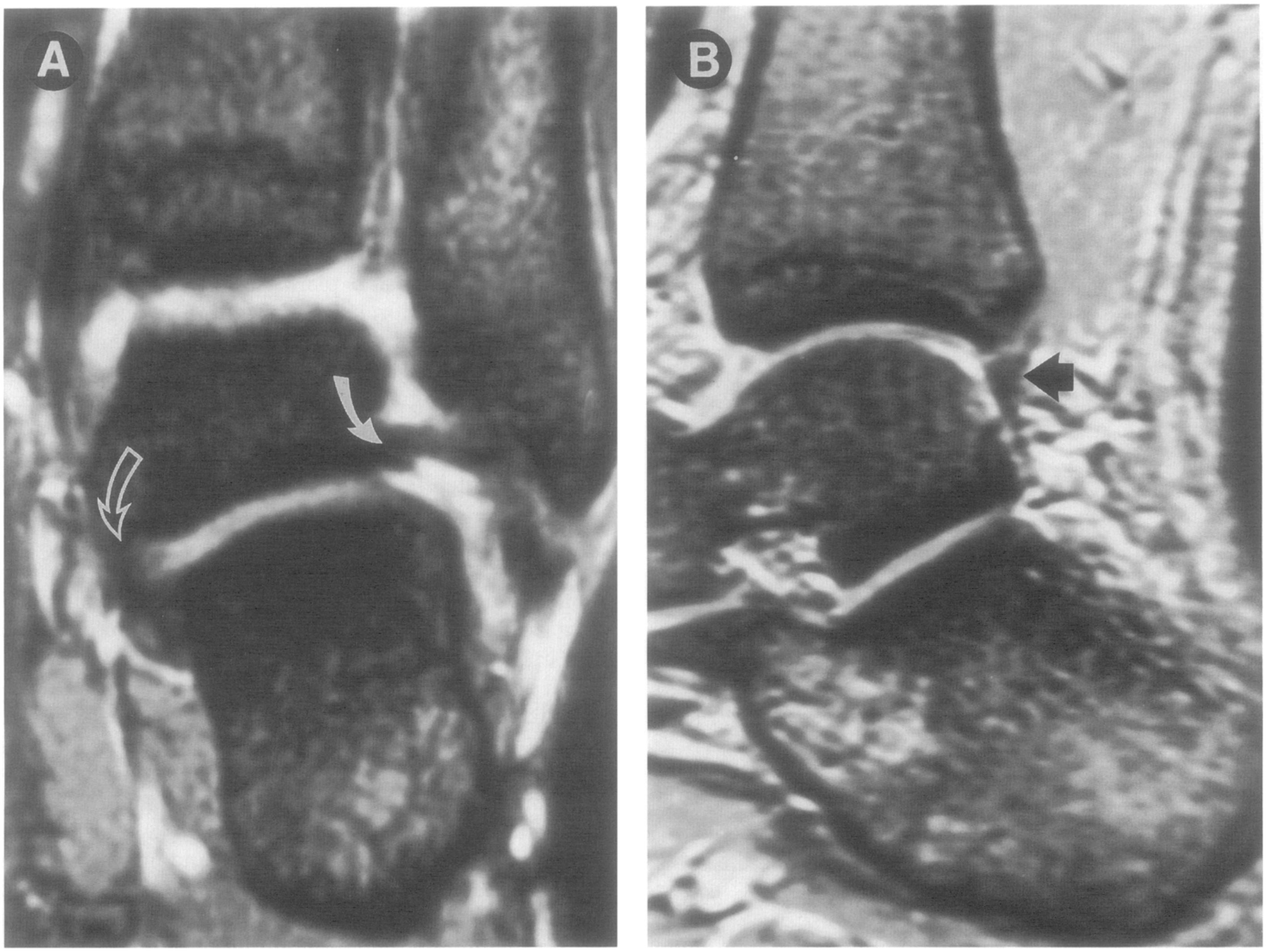

Fig 4. (A) Coronal gradient-echo image shows course of posterior talofibular ligament (PTFL, solid curved arrow) and posterior talocalcaneal ligament (open curved arrow). Note that hyaline cartilage is bright using gradient-echo imaging. (B) Sagittal gradient-echo image shows posterior talofibular (PTFL) ligament (arrow) as triangular-shaped low signal focus located posterior to talus. This structure can simulate a loose osteochondral body within the joint.

Complete acute disruptions usually have a gap between the retracted proximal and distal ends of the Achilles tendon.[6,14,17,19,21] Hemorrhage and edema at the site of the tear are bright on T2-weighted images and intermediate to low on T1-weighted images (Figs 10 and 11).[6,14,17,19,21] Acute partial tears do not have retracted ends and usually have bright signal at the site of the tear on T2-weighted images (Figs 10 and 11). Partial tears may be linear intrasubstance tears or incomplete transverse tears (Figs 10 and 11).[14,19,22] Partial intrasubstance tears have linear bands of bright signal on T2-weighted sequences but relatively smooth surface contour of tendon (Fig 10). A partial transverse tear is recognized by a segmental thinning or defect of the tendon substance with hemorrhage and edema within the defect of the partial (Fig 11). An intact plantaris tendon can be misinterpreted as a remaining strand of Achilles tendon but can be recognized by its typical location and by following its course on axial images (Fig 11).

Injuries of the anterior (extensor) tendons are less common than injuries of the flexor or peroneal groups but have a similar appearance and will not be displayed because of space limitations (Figs 1A and 7). Tendonitis, or rupture of the extensor tendons, is usually the result of repetitive dorsiflexion activities.

Peroneal Tendons

The peroneus brevis and peroneus longus share a common sheath within the peroneal tunnel as they pass posterior to the lateral malleolus in their course to the foot (Figs 7A and C).[23] The peroneal tendons are maintained with the canal by the superior and inferior peroneal retinacula.[23] Gradient-echo images using a three-dimensional Fourier transform technique can be reconstructed in the plane of the peroneal tendons and usually show that the tendons are of uniform width and homogenous dark signal (Fig 12).[24] Artifactual bright signal can be seen within normal peroneal and flexor tendons when they are oriented 55° in relation to the long axis of the magnet (Fig 13).[25] This "magic angle" artifact is most prominent on images using a short echo time such as T1-weighted spin-echo images and gradient-echo images and can be eliminated by plantar flexing the foot during imaging. Full-thickness tears of tendons frequently have a defect between the proximal and distal

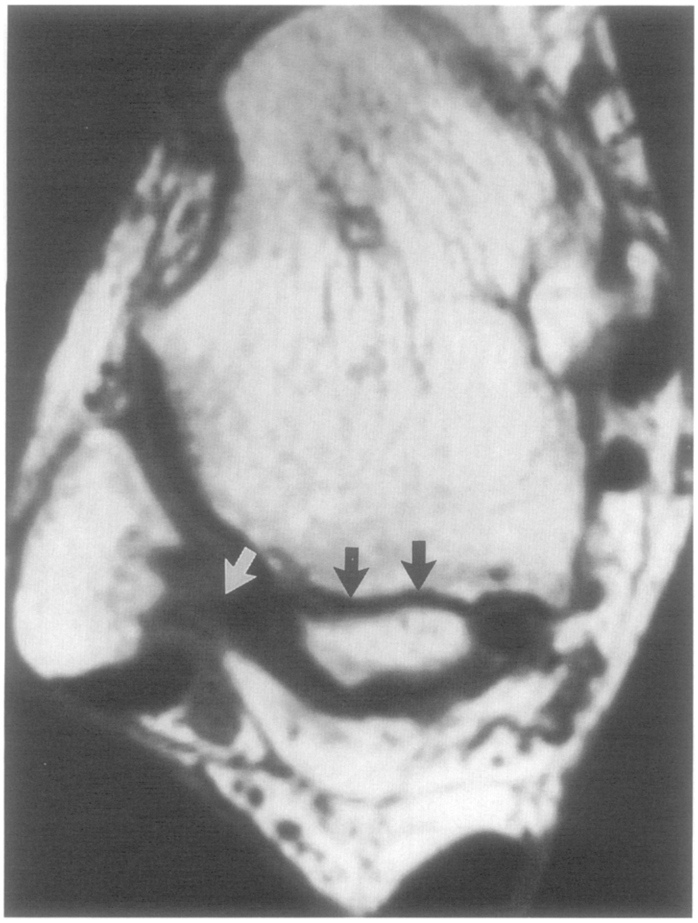

Fig 5. Axial T1-weighted spin-echo image (TR/TE = 600/20 ms) shows normal, bright marrow signal of os trigonum with smooth undulating synostosis with talar body (black arrows). Avulsion fracture of posterior process would have straight fracture line with low signal on T1-weighted images and bright signal of adjacent marrow on T2-weighted images. Posterior talofibular ligament attaches to os trigonum (white arrow).

fragments (Fig 14). The torn tendon is usually enlarged at the site of the tear and may have hemorrhage or edema (bright on T2-weighted images) at the site of the tear (Fig 14). Partial-thickness tears may be recognized by focal increased size associated with internal increased signal. In other cases, the partially torn tendon may separate into numerous fragments or strands (Fig 15). A tendon sheath effusion or tenosynovitis appears as bright signal within the tendon sheath on T2-weighted images (Fig 15). The peroneus longus tendon can be disrupted through an os peroneum (Fig 16).

Peroneal tendon dislocation usually results from disruption of the peroneal retinacula during an ankle inversion injury. Plain films may show a longitudinally oriented avulsion fracture of the fibula. MR imaging of the ankle while stressing the ankle (eversion and dorsi flexion) may be useful to document the etiology of the snapping sensation reported in patients with dislocating peroneal tendons (Fig 17).

Flexor Tendons and Tarsal Tunnel

The medial or flexor group of tendons are located posterior to the medial malleolus and are arranged from anterior to posterior: tibialis posterior, flexor digitorum longus, posterior tibial artery, posterior tibial vein, tibial nerve, and the flexor hallucis longus tendon (Figs 7A, B, and 18).[3] The three tendons and the posterior tibial neurovascular structures pass through a fibro-osseous canal called the tarsal tunnel as they pass on their way to the foot (Figs 7A, B, and 18).[26] The bony floor of the tarsal tunnel is formed by the medial surface of the talus, the sustentaculum talus, and the medial wall of the calcaneus (Figs 7A, B and 18).[26] The roof of the tunnel is formed by the flexor retinaculum arising on the anteromedial surface of the medial malleolus and inserting on the medial tuberosity of the calcaneus and the fascia overlying the abductor hallucis muscle (Fig 18).[26] The posterior tibial nerve is located behind the posterior tibial artery and anteromedial to the flexor hallucis longus tendon (Figs 7A, B, and 18).[3] The posterior tibial nerve gives off the medial calcaneal nerve and then divides into the medial and lateral nerves that are contained within separate fibrous subcompartments within the tarsal tunnel (Fig 19).[3,26-28] The medial calcaneal branch supplies innervation to the medial aspect of the heel.[3] The medial plantar nerve and vascular structures for the medial aspect of the foot are located within a dorsal compartment of the tarsal tunnel and travel just plantar and medial to the flexor hallucis longus tendon between the abductor hallucis and flexor digitorum brevis muscles (Fig 18).[3,26-28] The medial plantar nerve provides sensory innervation to most of the plantar aspect of the foot.[3] The lateral plantar nerve and associated vascular structures are enclosed within the plantar fibrous compartment that passes between the flexor digitorum brevis and quadratus plantae muscles (Fig 18).[3,26-28] The lateral plantar nerve provides sensory innervation to the lateral aspect of the foot and innervates many of the intrinsic muscles of the foot.[3]

Tarsal tunnel syndrome is a clinical entity characterized by burning pain in the toes, sole of the foot, or medial heel that is aggravated by weightbearing.[29,30] The tarsal tunnel syndrome is caused by entrapment of the posterior tibial nerve or its branches and may have numerous etiologies that either restrict the volume of the tarsal tunnel or impress on the posterior tibial nerve or its branches. Common etiologies include, ganglion cysts (Fig 19), tenosynovitis of the flexor tendons with tendon sheath effusions (Fig 20), venous varicosities, hindfoot valgus, or posttraumatic fibrosis of the tarsal tunnel (Fig 21).[26-28] Erickson et al[26] have described the usefulness of an oblique axial imaging plane to examine the tarsal tunnel (Fig 22).

The posterior tibial tendon passes just posterior to the medial malleolus, deep to the flexor retinaculum, and superficial to the deltoid ligament during its course to insertions into the navicular tuberosity and base of the medial cuneiform (Figs 7 and 18).[3] The flexor digitorum longus follows a similar course just posterior to the tibialias posterior tendon during its course to the insertions into the plantar bases of the second to fifth distal phalanges (Figs 7 and 18).[3] The flexor hallucis longus tendon is located lateral to the other two tendons of the flexor group and passes through its own fibro-osseous canal along the postero-medial talus, beneath the sustentaculum talus, and between the abductor hallucis and flexor digitorum brevis muscles (Figs 17 and 18).

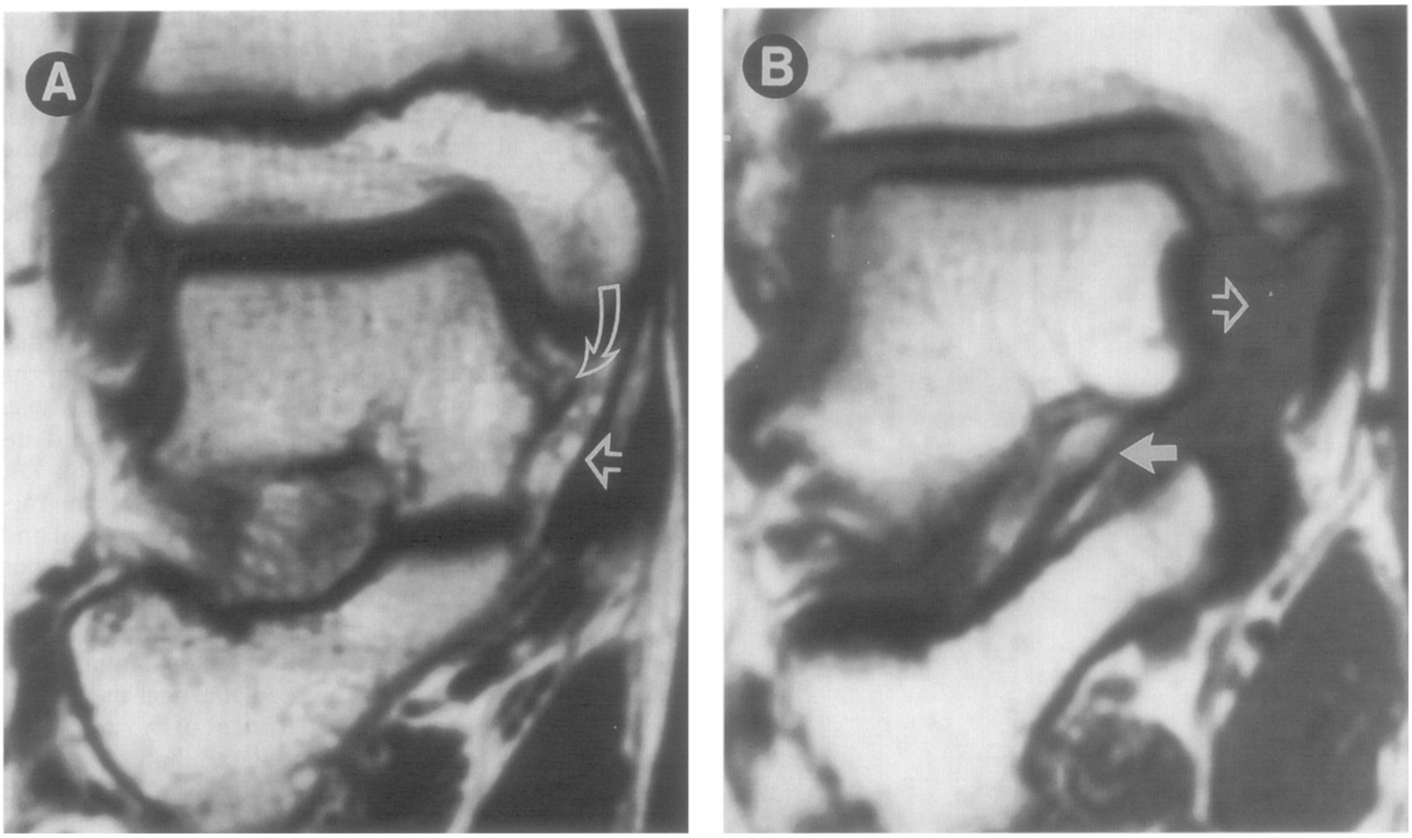

Fig 6. (A) Coronal T1-weighted image shows superficial deltoid ligament (straight open arrow) attaching medial malleolus to sustentaculum talus and deep deltoid ligament (curved open arrow) attaching to medial aspect talus. (B) Coronal T1-weighted image shows disruption of superficial and deep deltoid fibers (open arrow) following ankle eversion injury. Talocalcaneal interosseous ligament (closed arrow) supports the subtalar joint along with the cervical ligament.

Injury of the posterior tibial tendon is the most frequently recognized injury of the three flexor tendons.[31-33] Tears of the posterior tibial tendon are thought to be the result of repeated microtrauma, leading to tendon degeneration, tendonitis, and eventually complete tears.[34] Rosenberg et al[32] classified the imaging features of posterior tibial tendon tears into three types: type 1–partial tear with focal areas of fiber rupture, degeneration, and repair and characterized by focal tendon enlargement and increased signal on T1-weighted images (Fig 23); type 2–focal decreased width of the tendon representing partial tear with attenuation (usually at the level of the posterior malleolus); and type 3–discontinuity of the tendon consistent with complete rupture. Tendon discontinuity, marked focal enlargement, or thinning of the posterior tibial tendon are still considered reliable signs of posterior tibial tendon tears but recent investigation of asymptomatic volunteers have shown a normal overlap in the width and signal characteristics of patients with tears of the posterior tibial tendon and asymptomatic volunteers.[35]

FRACTURES

Sports-related fractures of the foot and ankle may be secondary to acute trauma or repetitive stress or overuse. Most of the acute fractures produced during sporting events are not unique (ie, fractures of the ankle, fifth metatarsal, digits); however, some fractures may be hard to diagnose clinically and are worthy of mention because of their unique appearances on imaging studies.

Radiographically, occult fractures of the talar dome are frequently discovered during MR imaging of patients with pain after an athletic injury. MR imaging is a sensitive test for detecting osteochondral lesions of the talar dome and can accurately evaluate for osteochondral detachment. Gradient-echo images are useful for evaluating the integrity of the hyaline cartilage overlying the osteoarticular fragment and the presence of fluid signal beneath the osteoarticular fragment is a reliable sign of fragment displacement (Fig 24).[36]

Fractures of the talar body and processes can be diagnosed using plain radiographs but have been recognized more frequently using MR imaging (Fig 25). Fractures of the talar body are usually considered to be the result of high-energy trauma; however, we have seen a few radiographically occult fractures of the talar body using MR imaging that were produced from sporting injuries (Fig 25). In these cases, MR imaging showed the fracture line as a linear band of low signal on all sequences surrounded by marrow edema (dark on T1-weighted images, bright on T2-weighted images).

Fractures of the lateral process occur during ankle inversion injury.[37] These fractures are frequently missed when the patient presents to the emergency room because the fracture line is obscured by overlying bony structures (Figs 26 and 27). Most lateral process fractures are diagnosed weeks after the initial injury when

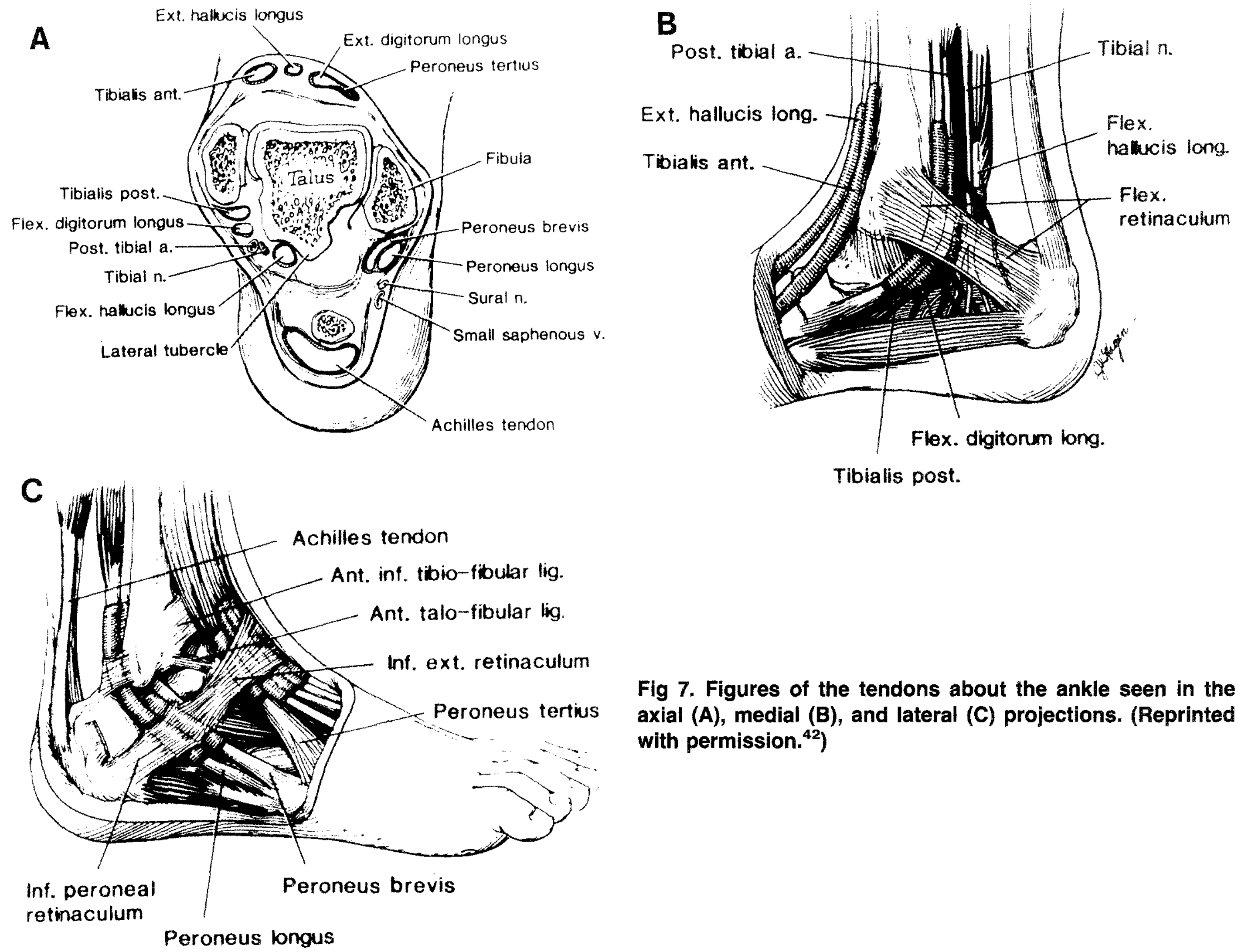

Fig 7. Figures of the tendons about the ankle seen in the axial (A), medial (B), and lateral (C) projections. (Reprinted with permission.[42])

the patient returns with persistent ankle pain. The fracture line is readily visualized using complex motion tomograms, computed tomography (CT), or MR imaging (Figs 26 and 27).

Avulsion fractures of the anterior process of the calcaneus by the bifurcate ligament are produced during an ankle inversion injury and represent 15% of recognized calcaneal fractures.[38,39]

They are usually not recognized on the initial series of radiographs when the patient presents to the emergency room (Fig 28). The fracture is usually identified on the oblique view of the foot or lateral view of the ankle when the patient returns with persistent pain (Fig 28).[38,39] The fracture can be easily shown using complex motion, CT, or MR imaging although most of these fractures can be identified using plain radiographs if the examiner carefully evaluates this location on all radiographs obtained after an ankle inversion injury.

Stress fractures are common injuries in athletes. In a series of 320 stress fractures in athletes, Matheson et al[40] found that the tibia was involved in 49%, the tarsal bones in 25%, the metatarsals in 9%, the fibula in 7%, and the sesamoid bones in less than 1%. Stress fractures of the distal tibia are usually transversely oriented and located at the metaphyseal/diaphyseal junction (Fig 29) MR imaging usually shows the fracture line along with associated marrow edema and adjacent soft-tissue edema. Some stress fractures (especially those of the medial malleolus) will appear as marrow edema on T2-weighted images and the fracture line may not be seen (Fig 30).

Stress fractures of the tarsal navicular may be difficult to recognize using plain radiographs because of the overlap of adjacent bones (Fig 31). Most navicular stress fractures are oriented in the sagittal plane and involve the central or medial third of the bone. In problem cases, either MR or CT may be used to show the fracture (Fig 31).

Some injuries produce chronic pain but are of uncertain etiology. A basketball player with previous ankle injuries presented with acute exacerbation (Fig 32). Bone scan showed increased uptake of the posterior process of the talus. MR examination marrow and soft-tissue fibrosis adjacent to the medial process of the talus but no definite fracture. CT examination showed a curvilinear calcification adjacent to the medial process that may have been an avulsion of posttraumatic calcification.

Special imaging can be extremely helpful in making the correct diagnosis of sports related injuries. I cannot overemphasize the importance of communicating with the skeletal radiologist when referring patients for imaging. The optimal imaging modality for one entity may be very poor for another pathologic entity. If the history

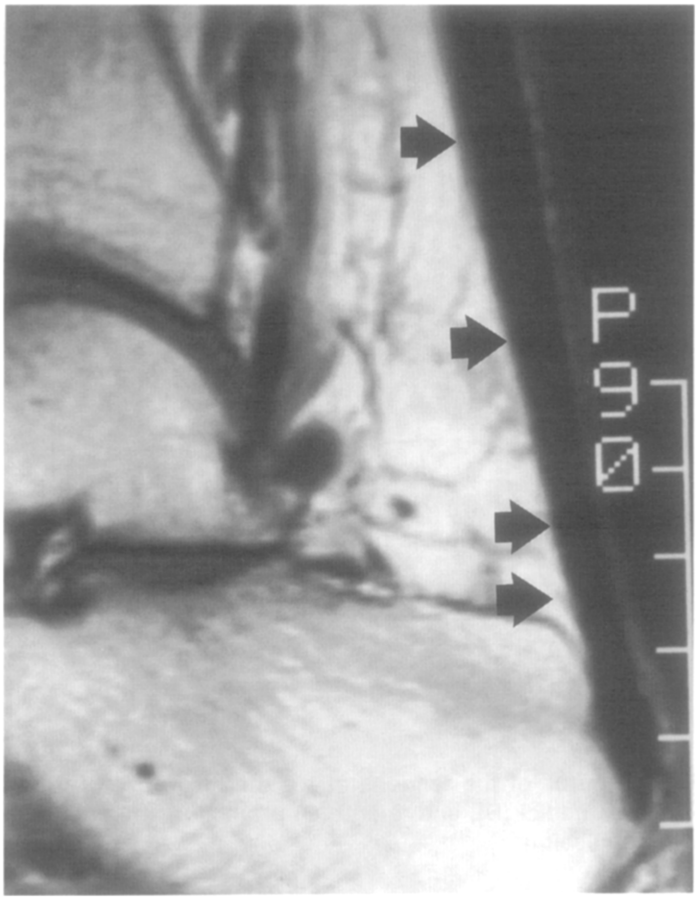

Fig 8. Sagittal T1-weighted image (TR = 600 ms, TE = 20 ms) shows uniform black signal in Achilles tendon originating from the confluence of the gastrocnemius and soleus muscles and inserting into the os calcis. Tendon smoothly tapers from the origin to insertion without defect, enlargement, or signal inhomogeneity (arrows).

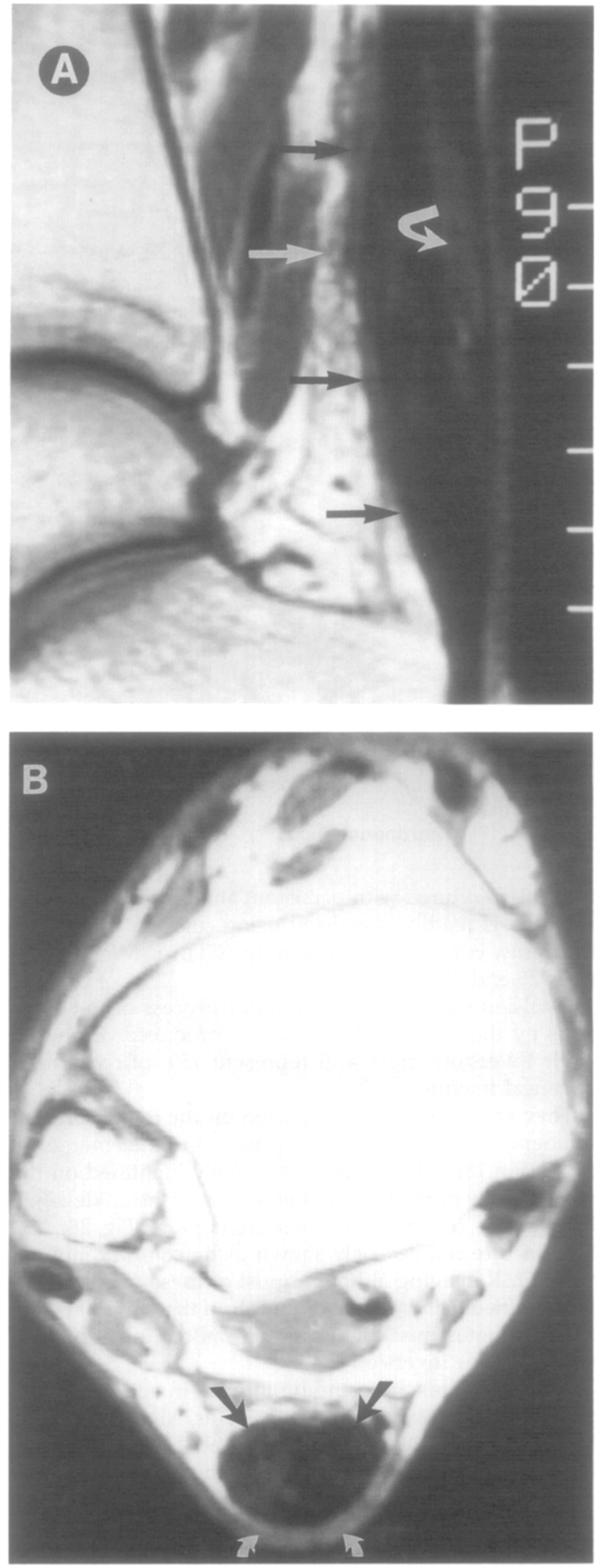

Fig 9. (A) Sagittal T1-weighted image (TR = 600 ms, TE = 20 ms) shows fusiform enlargement of the Achilles tendon (black arrows) with linear bands of intermediate (gray) signal representing partial intra-substance tears (curved white arrow). Stranded low signal in fat plane anterior to Achilles tendon represents edema (straight white arrow). (B) Axial T1-weighted image (TR = 600 ms, TE = 20 ms) just proximal to tibial plafond shows patchy intermediate (gray) signal within an enlarged Achilles tendon (black arrows) consistent with chronic tendonitis and internal degeneration. Intermediate (gray) signal within subcutaneous fat represents chronic fibrosis (white arrows).

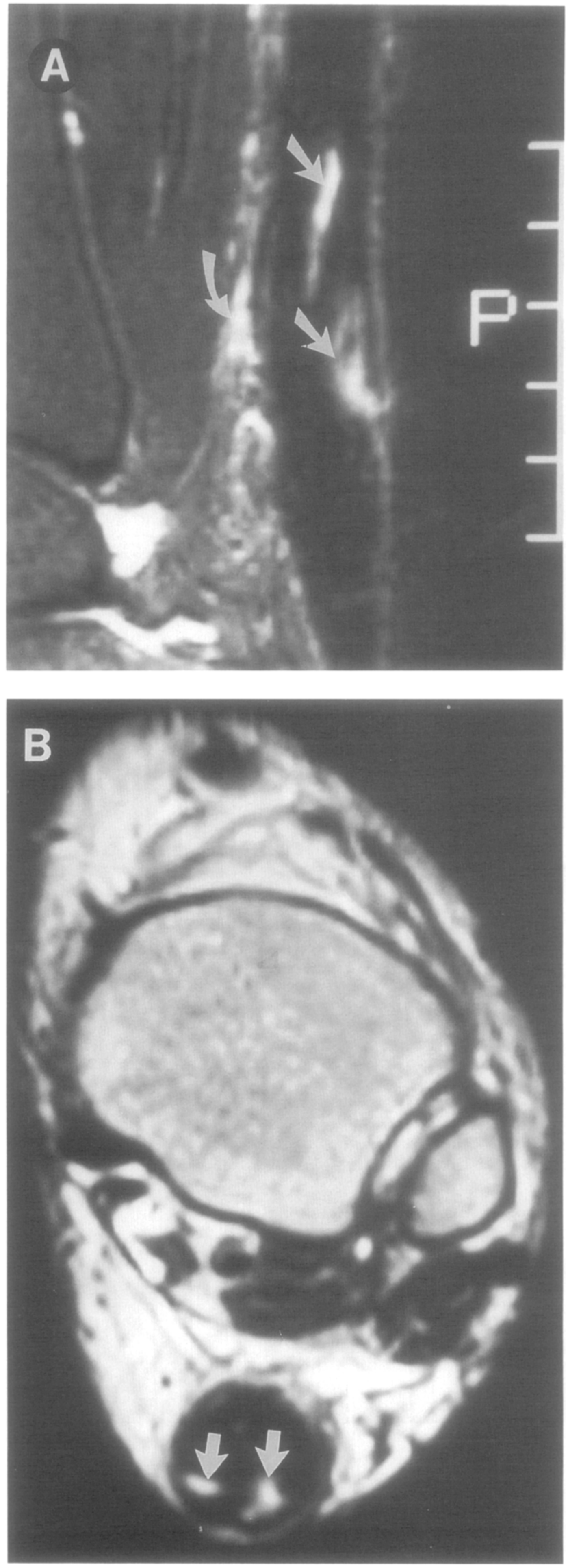

Fig 10. (A) Sagittal fast-spin echo T2-weighted image shows linear bright signal within partial-thickness, intrasubstance tears (oblique arrows) and pre-Achilles soft-tissue edema (curved arrow). (B) Axial fast-spin echo T2-weighted image shows bright intrasubstance tears (arrows).

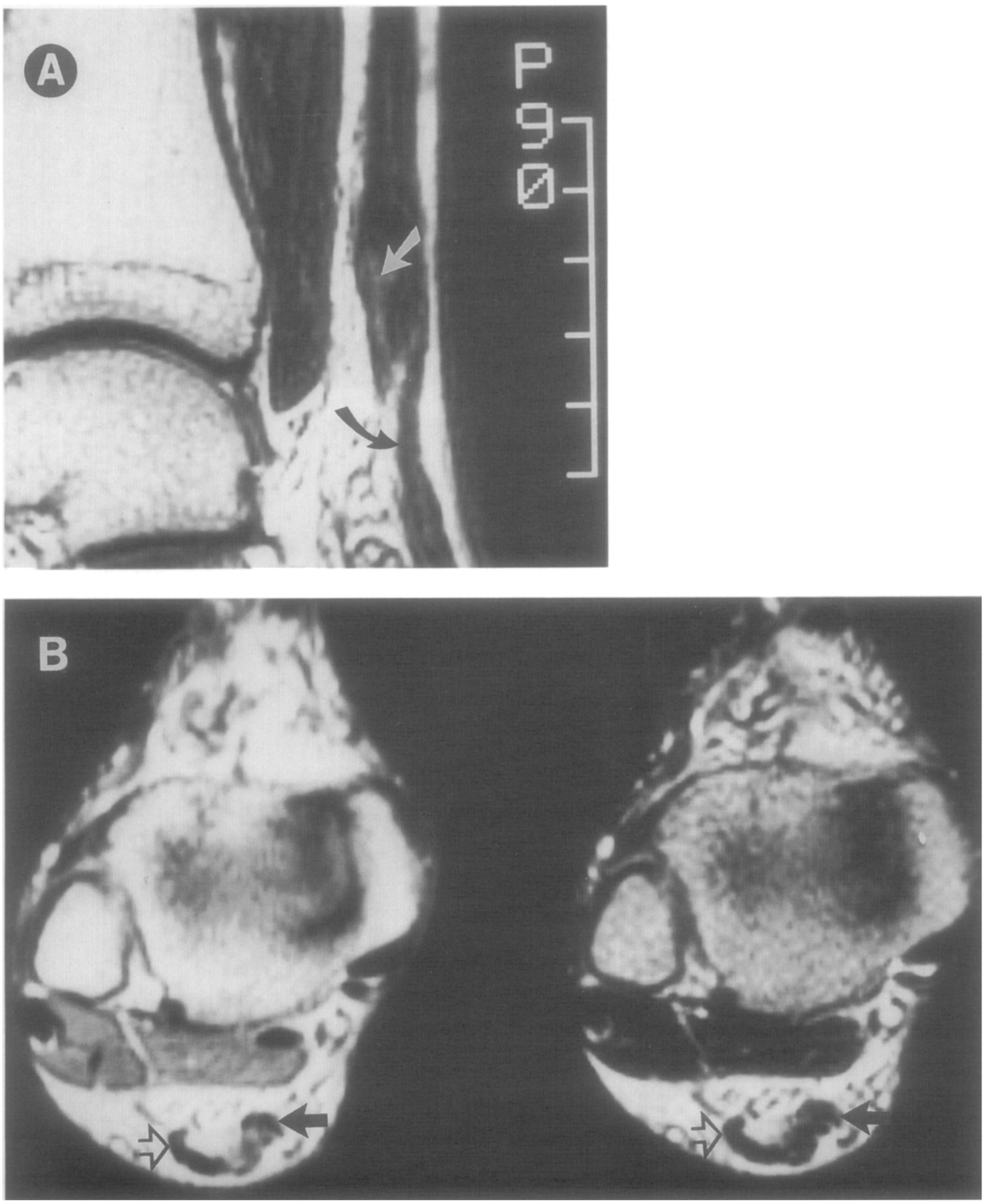

Fig 11. (A) Sagittal T1-weighted image (TR = 600 ms, TE = 20 ms) shows incomplete tear of Achilles tendon located 3 cm above insertion into os calcis with thin strand of intact tendon (curved black arrow). Proximal fragment is enlarged with internal high signal hemorrhage (white arrow: bright on T1-weighted image). (B) Axial proton-density weighted (left: TR/TE = 2,000/20 ms) and T2-weighted (right: TR/TE = 2,000/80 ms) sequences show intact plantaris tendon (closed black arrow) and small portion of Achilles tendon (open arrow) with torn Achilles tendon tissue with intermediate (gray) signal intensity.

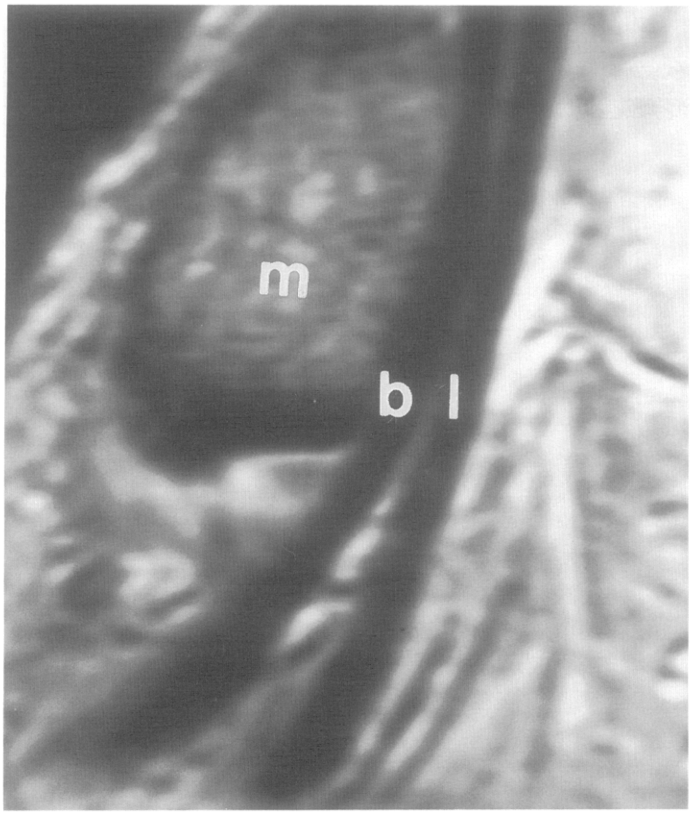

Fig 12. Reconstructed oblique sagittal image (TR/TE/flip = 37/min/15°) in long axis of peroneal tendons shows uniform thickness and homogenous black signal. Peroneus brevis (b) tendon is located just posterior to lateral malleolus (m) and anterior to peroneus longus (l) tendon.

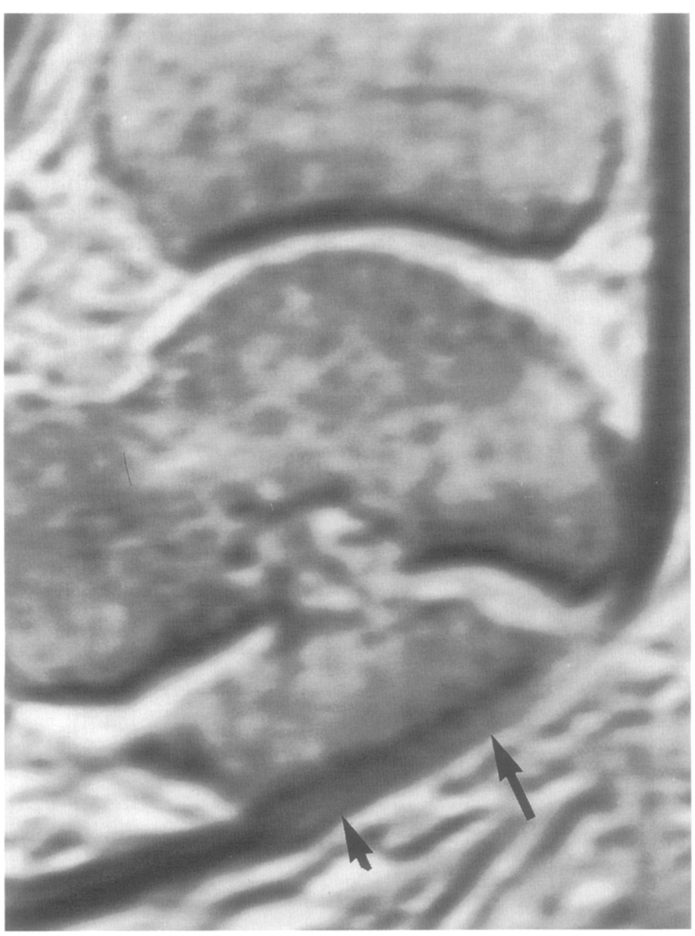

Fig 13. Reconstructed oblique sagittal image (TR/TE/flip = 37/min/15°) in long axis of flexor hallucis longus tendon shows artifactual bright signal ("Magic angle" phenomenon) within normal FHL as it passes beneath sustentaculum talus (arrows). Partial-thickness tear would also have internal signal that is usually enlarged.

Fig 14. Reconstructed oblique sagittal image shows full-thickness tear of peroneus brevis tendon with smooth enlargement and abrupt cut-off at the site of tear.

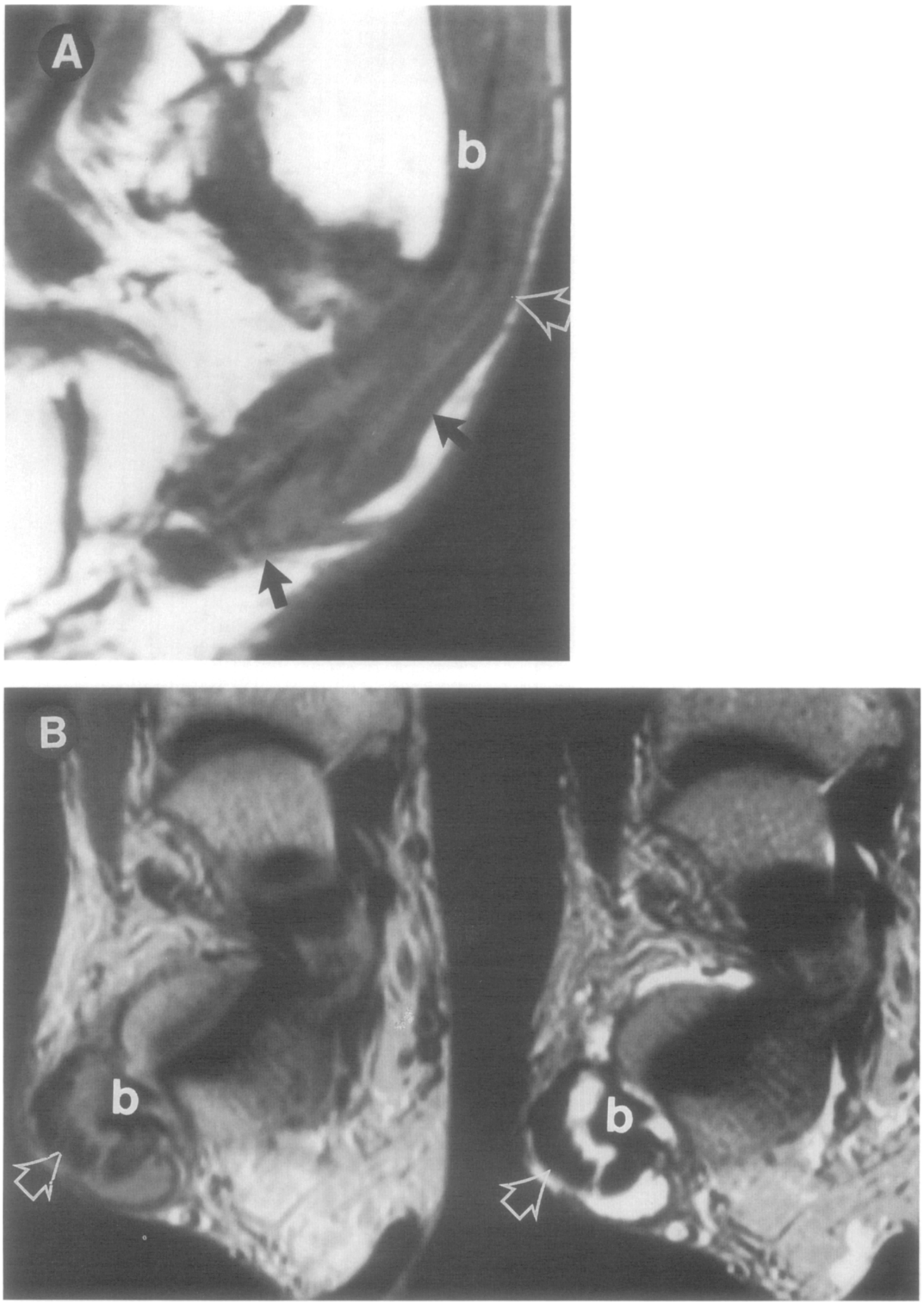

Fig 15. (A) Oblique sagittal T1-weighted spin-echo image shows partial-thickness tears of peroneus longus tendon with marked enlargement and diffusely increased signal compared with peroneus brevis tendon (b). (B) Axial proton-density weighted (left) and T2-weighted (right) spin-echo images show normal size and appearance of peroneus brevis (b) tendon and marked enlargement of peroneus longus tendon that is fragmented into several slips (open arrow). Tendon slips are surrounded by fluid representing tenosynovitis. (Courtesy of Jim Gilley, MD, San Antonio, TX.)

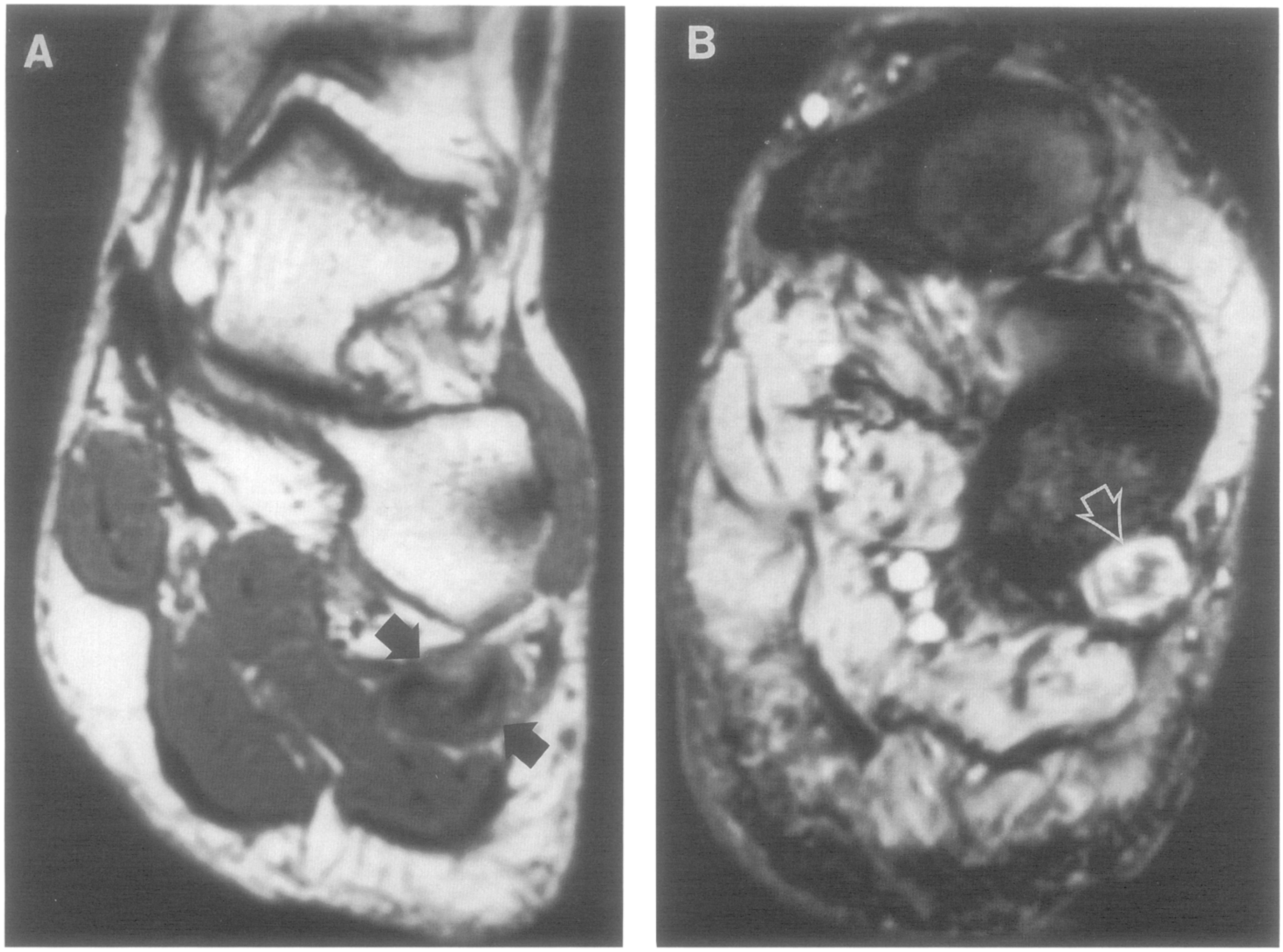

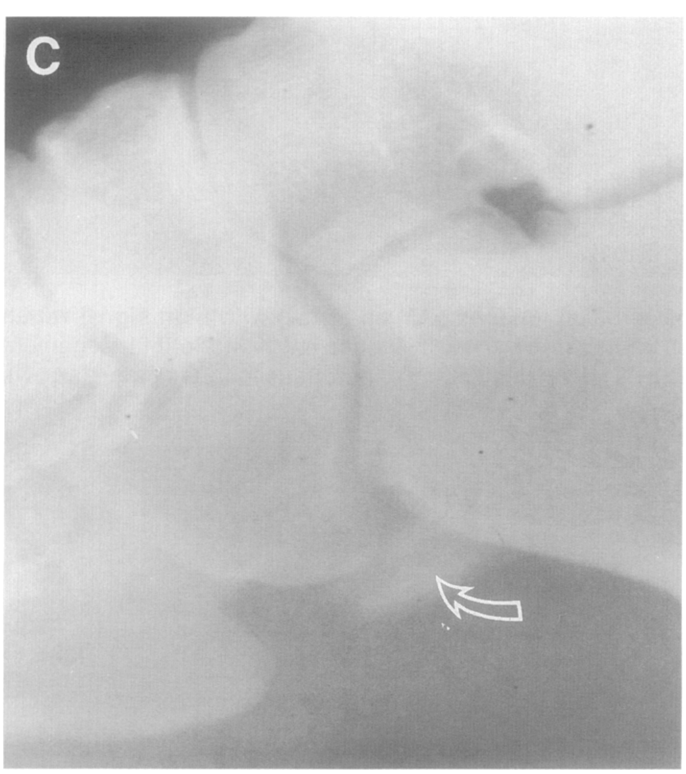

Fig 16. (A) Coronal T1-weighted spin-echo sequence shows an enlarged peroneal longus tendon with mixed signal intensity (between arrows) of fractured os peroneum. (B) Coronal gradient-echo image shows high signal surrounding peroneal tendon (open arrow). (C) Lateral radiograph shows distal fracture of os peroneum in same patient. (Courtesy of Jim Gilley, MD, San Antonio, TX.)

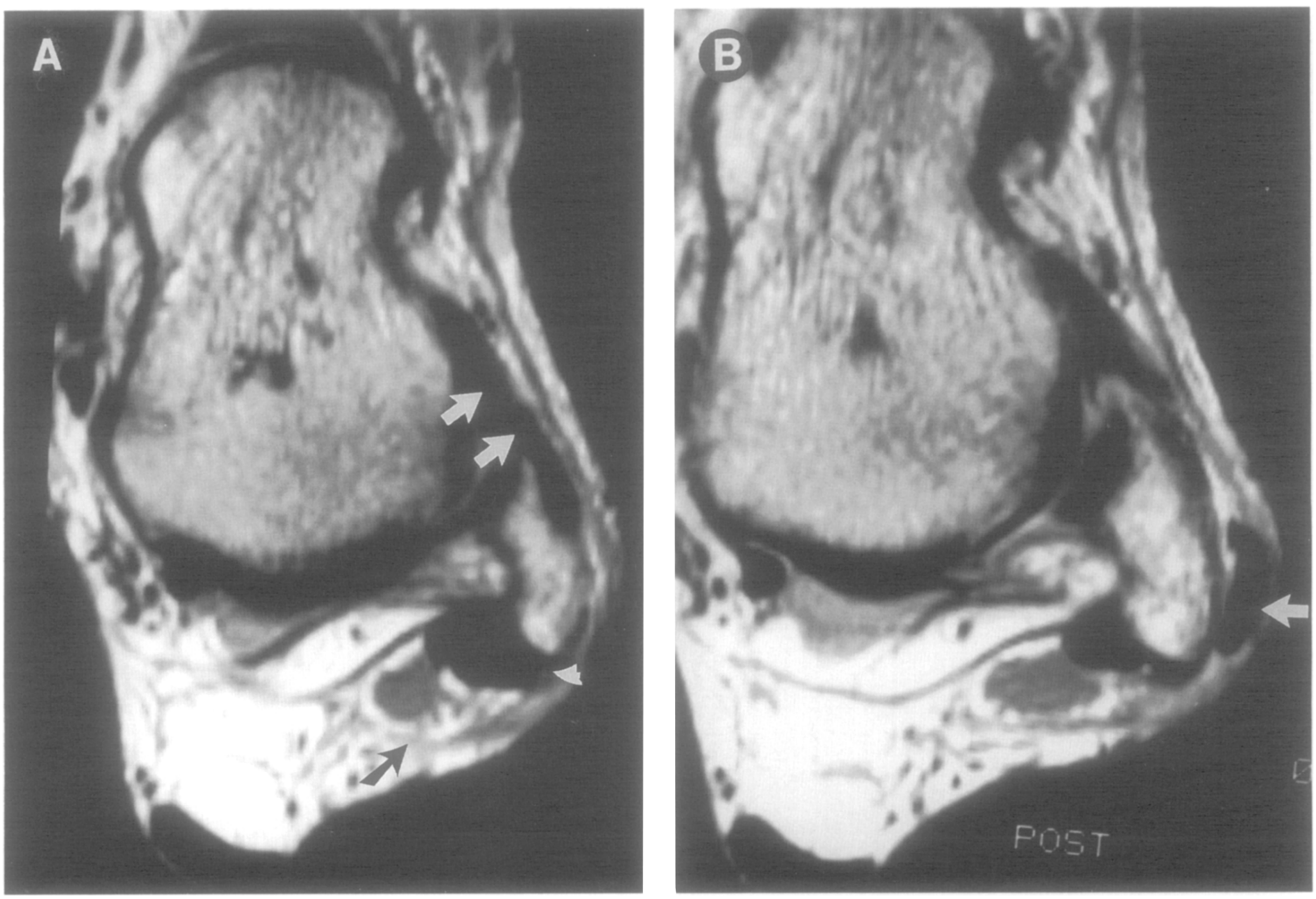

Fig 17. (A) Axial T1-weighted image shows normal orientation of peroneal tendons (curved arrow) with high signal within lateral aspect of peroneal retinaculum (medial margin-black arrow). White arrows show thickened anterior talofibular ligament from old injury. (B) Stress view with eversion and flexion of ankle shows lateral dislocation of peroneus longus tendon (arrow). (Courtesy of Jim Gilley, MD, San Antonio, TX.)

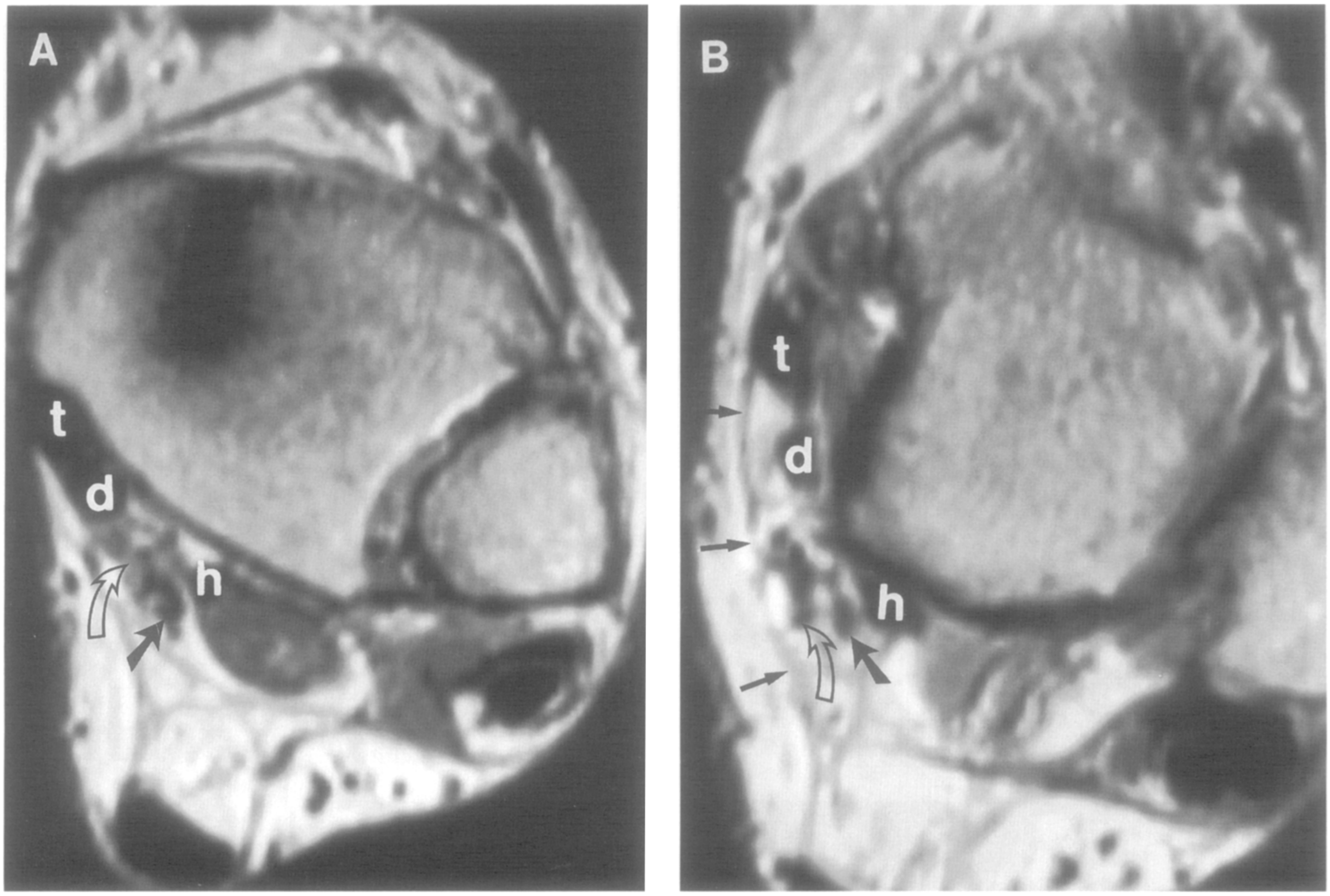

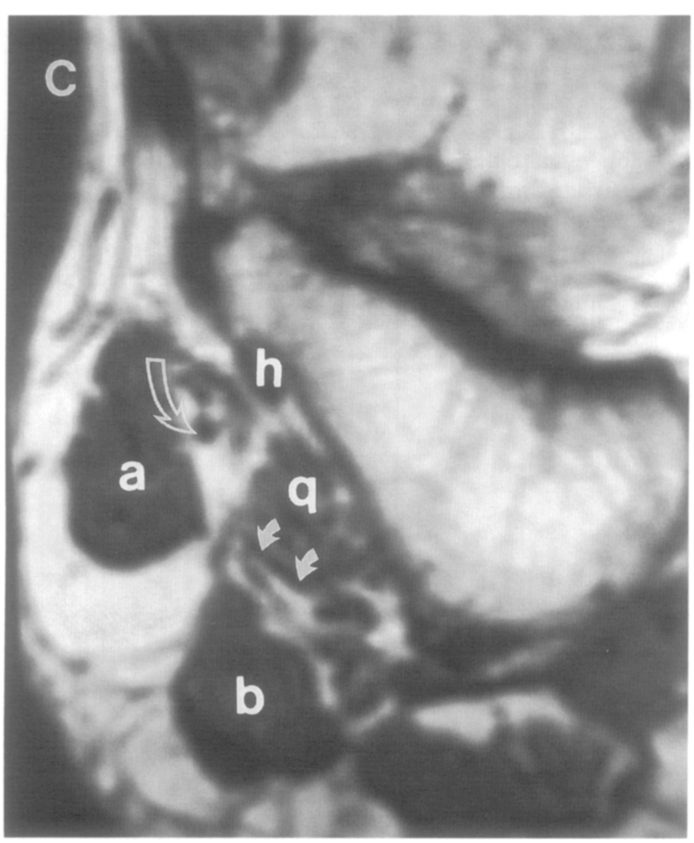

Fig 18. (A) Axial T1-weighted image at level of distal tibial and fibular joint shows posterior tibial tendon (t), flexor digitorum tendon,[41] posterior tibial neurovascular bundle (curved open arrow), tibial nerve (closed arrow), and flexor hallucis longus tendon. (B) Axial T1-weighted image through upper portion of tarsal tunnel shows roof formed by flexor retinaculum (small black arrows) and floor formed by medial surface of talus. Curved open arrow, medial plantar nerve; large solid arrow, lateral plantar nerve. (C) Coronal T1-weighted image at level of sustentaculum talus shows medial plantar nerve (open arrow) located medial and plantar to flexor hallucis longus tendon (H). Lateral plantar nerve (small curved arrows) follows course of flexor digitorum tendon between quadratus plantae (q) and flexor digitorum brevis (b) muscles.

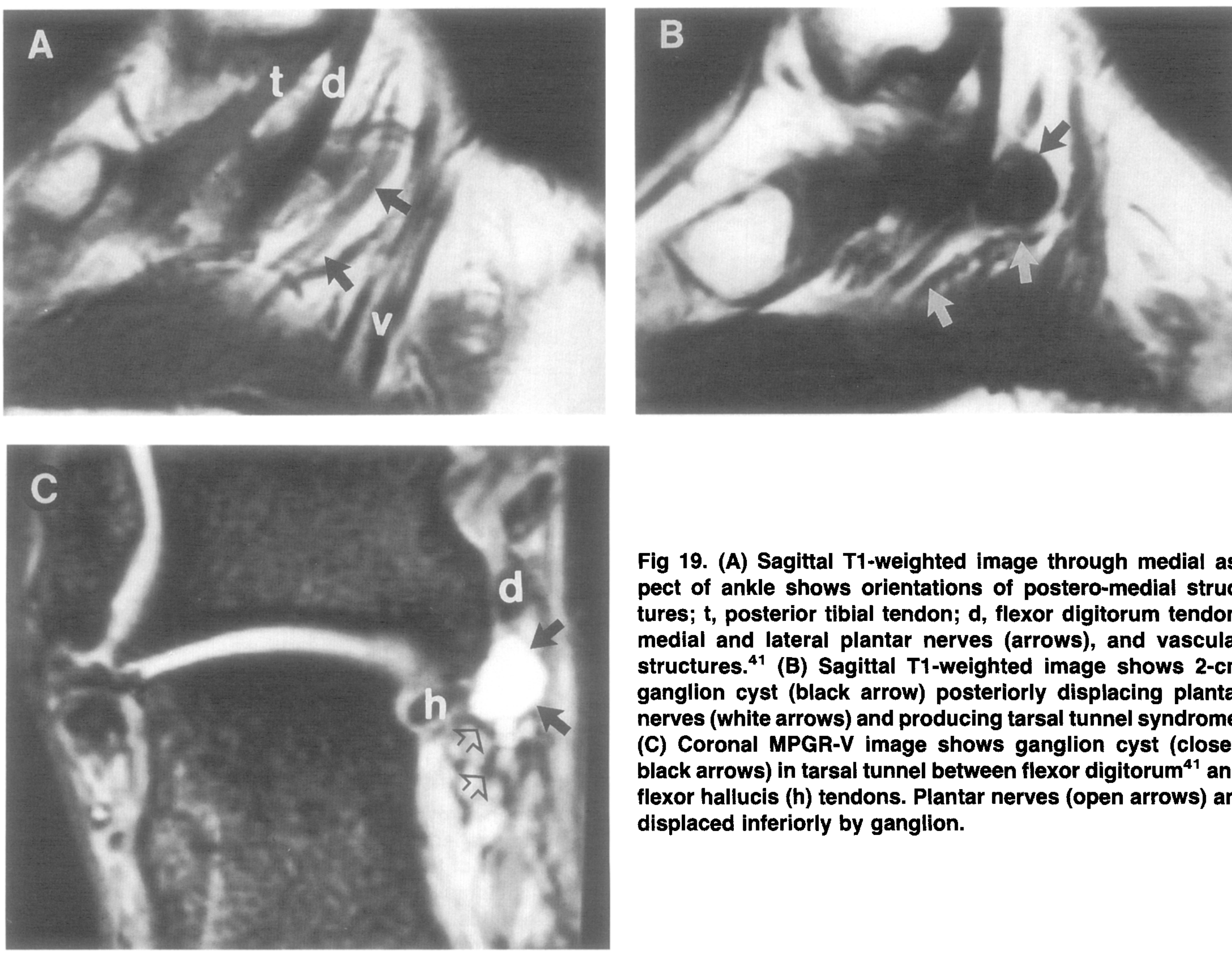

Fig 19. (A) Sagittal T1-weighted image through medial aspect of ankle shows orientations of postero-medial structures; t, posterior tibial tendon; d, flexor digitorum tendon, medial and lateral plantar nerves (arrows), and vascular structures.[41] (B) Sagittal T1-weighted image shows 2-cm ganglion cyst (black arrow) posteriorly displacing plantar nerves (white arrows) and producing tarsal tunnel syndrome. (C) Coronal MPGR-V image shows ganglion cyst (closed black arrows) in tarsal tunnel between flexor digitorum[41] and flexor hallucis (h) tendons. Plantar nerves (open arrows) are displaced inferiorly by ganglion.

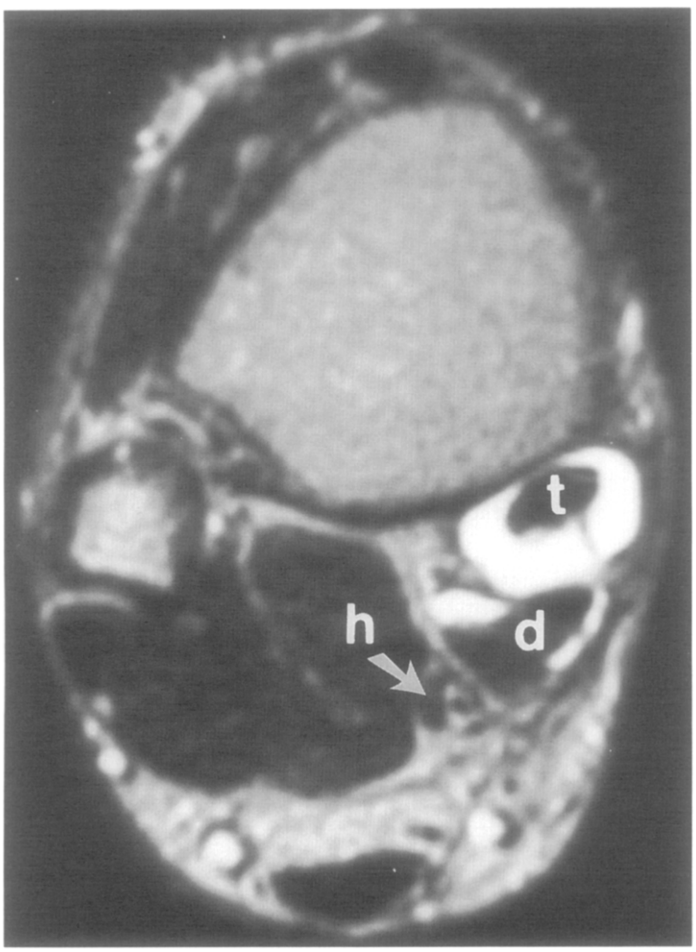

Fig 20. Axial fast-spin echo T2-weighted image (TR/TE = 3,000/108 ms) shows posterior tibial tendon (t) surrounded by fluid. d, flexor digitorum tendon; H, flexor hallucis longus muscle; white arrow, tibial nerve.

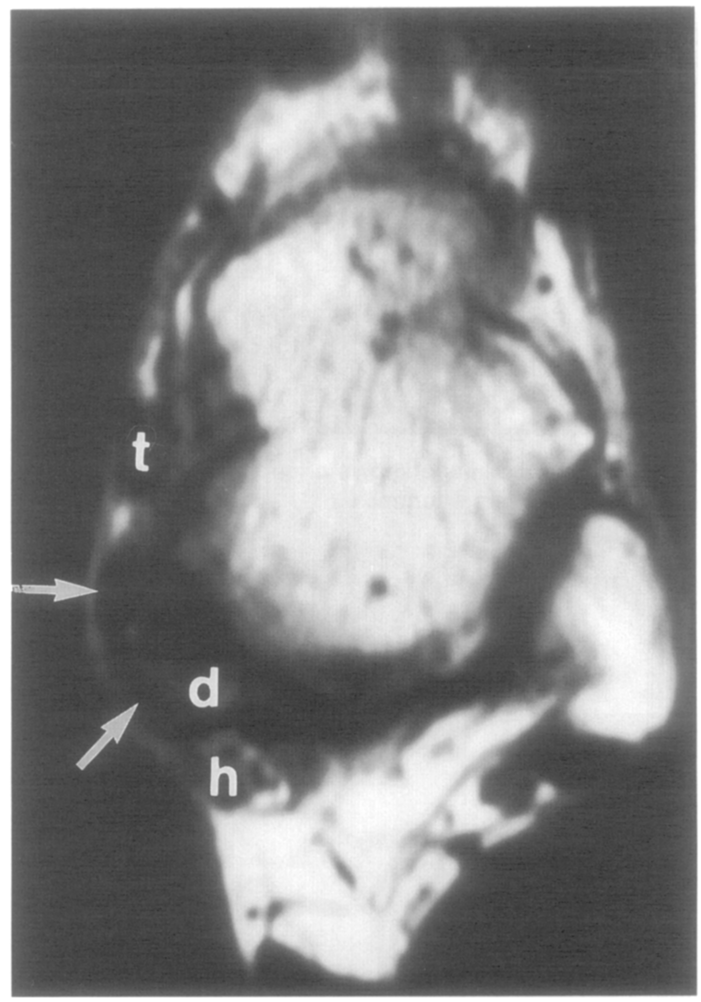

Fig 21. Axial T1-weighted image shows thickened flexor retinaculum (arrows) with fibrosis (low signal) within tarsal tunnel surrounding flexor digitorum tendon[41] and producing tarsal tunnel syndrome. T, posterior tibial tendon; h, flexor hallucis longus tendon.

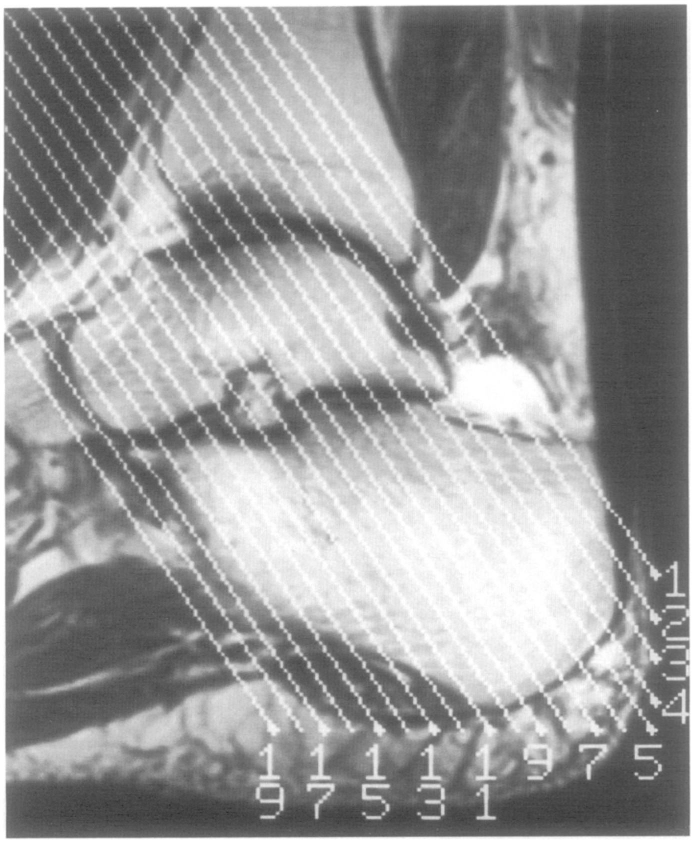

Fig 22. Reference image shows orientation of oblique axial images through tarsal tunnel.

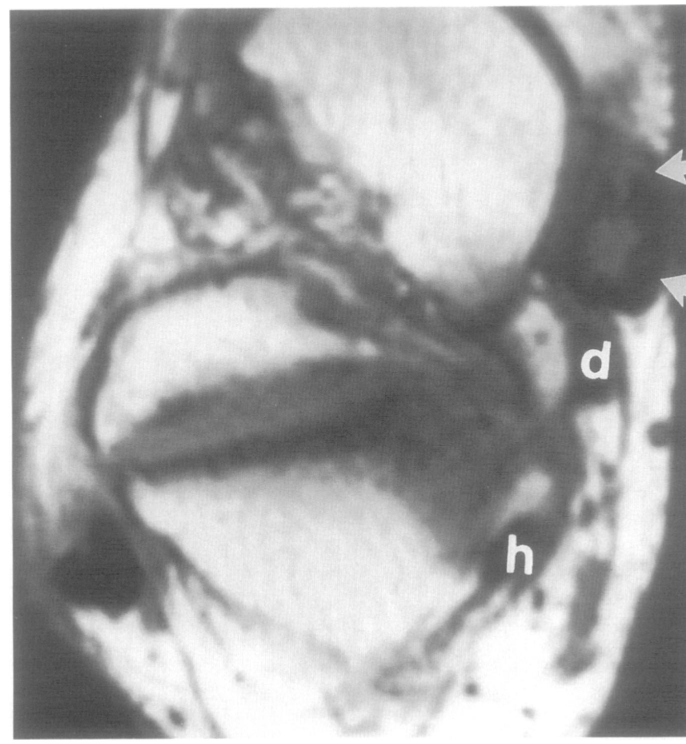

Fig 23. Sagittal T1-weighted image shows enlarged posterior tibial tendon with intermediate signal consistent with chronic inflammation and partial tear (arrows). d, flexor digitorum longus tendon; h, flexor hallucis longus tendon.

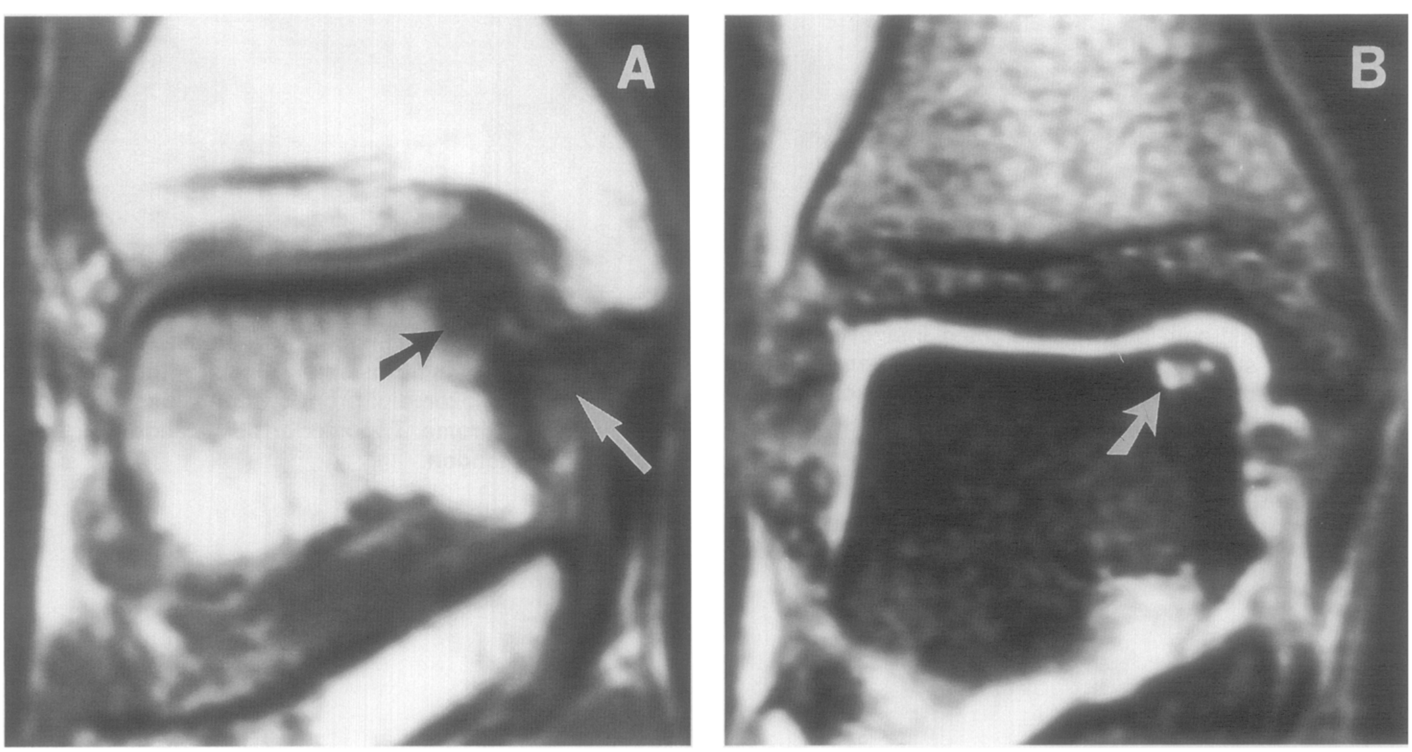

Fig 24. (A) Coronal T1-weighted image shows low signal (sclerosis) of subchondral bone of medial talar dome (oblique arrow). Deep deltoid ligament (white arrow) is not well seen consistent with previous tear. (B) First echo of multiphasic, gradient-recalled, multiecho, multiplanar (MPGR-V) image shows subchondral cystic change of medial talar dome with intact overlying hyaline cartilage (no evidence of detachment).

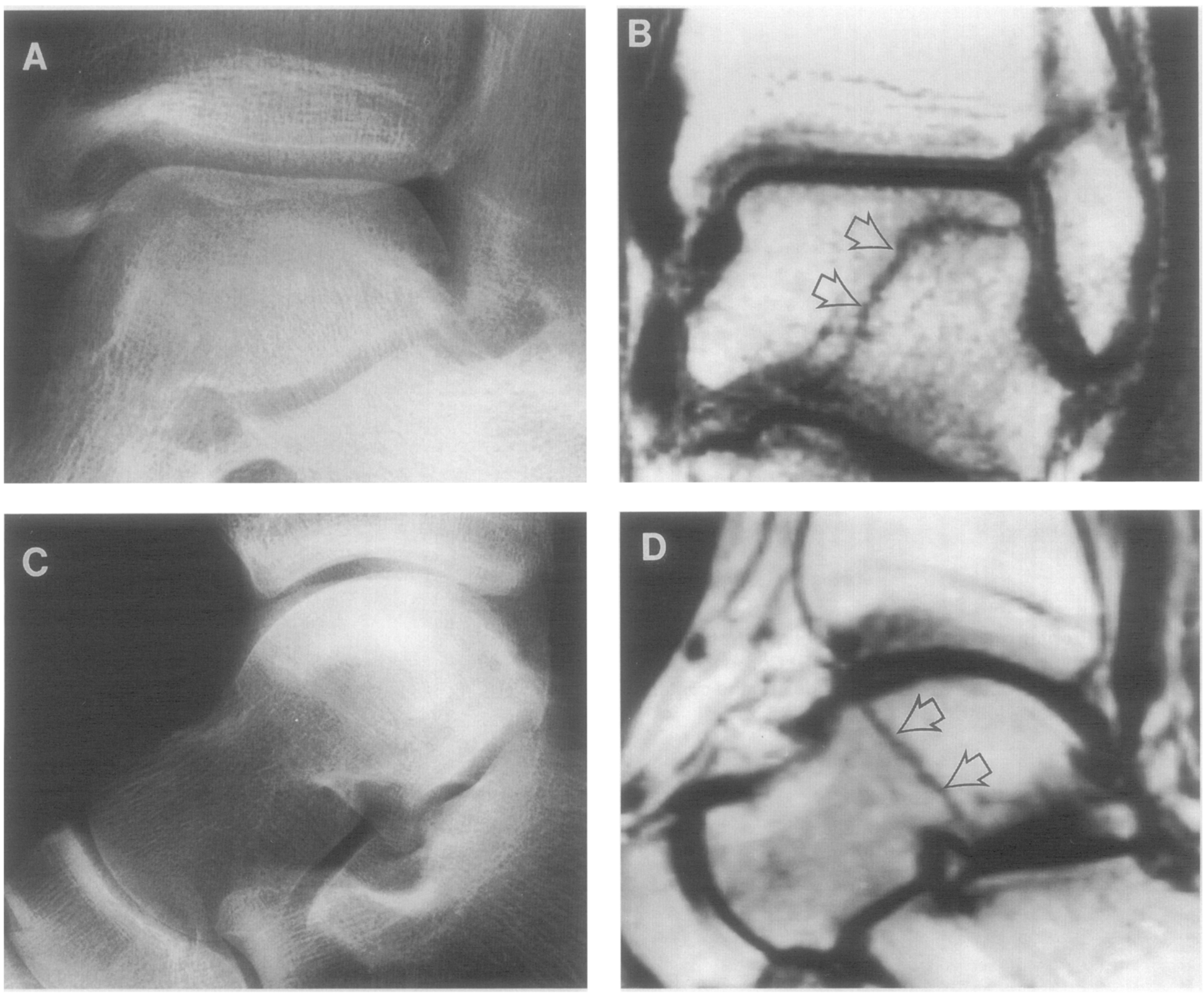

Fig 25. (A) Normal frontal radiograph of ankle of young man with ankle pain after jumping injury. (B) Coronal T1-weighted spin-echo image (TR/TE = 600/20 ms) shows obliquely oriented fracture line (open arrows) through talar body. (C) Normal lateral radiograph. (D) Sagittal T1-weighted spin-echo image (TR/TE = 600/20 ms) shows obliquely oriented fracture line (open arrows) through talar body. (Courtesy of Jim Gilley, MD, San Antonio, TX.)

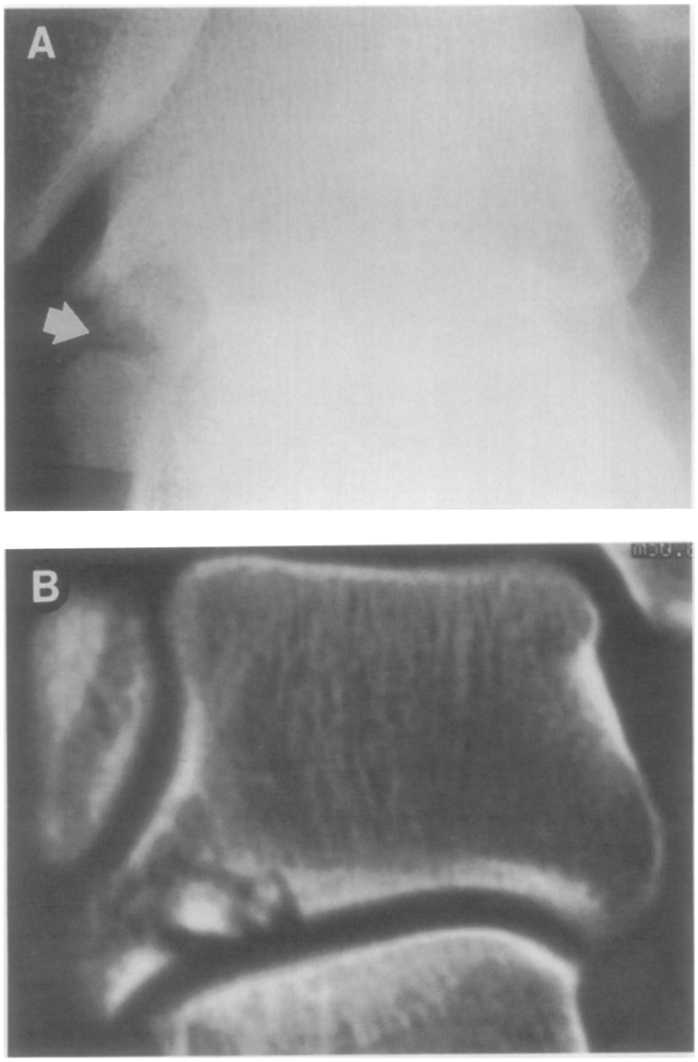

Fig 26. (A) Frontal radiograph shows oblique fracture line through lateral process of talus (arrow). (B) Coronal CT slice shows that lateral process fracture extends into the posterior facet of the subtalar joint.

Fig 28. Lateral radiograph shows displaced avulsion fracture involving anterior process of calcaneus (arrow) at site of bifurcate ligament insertion.

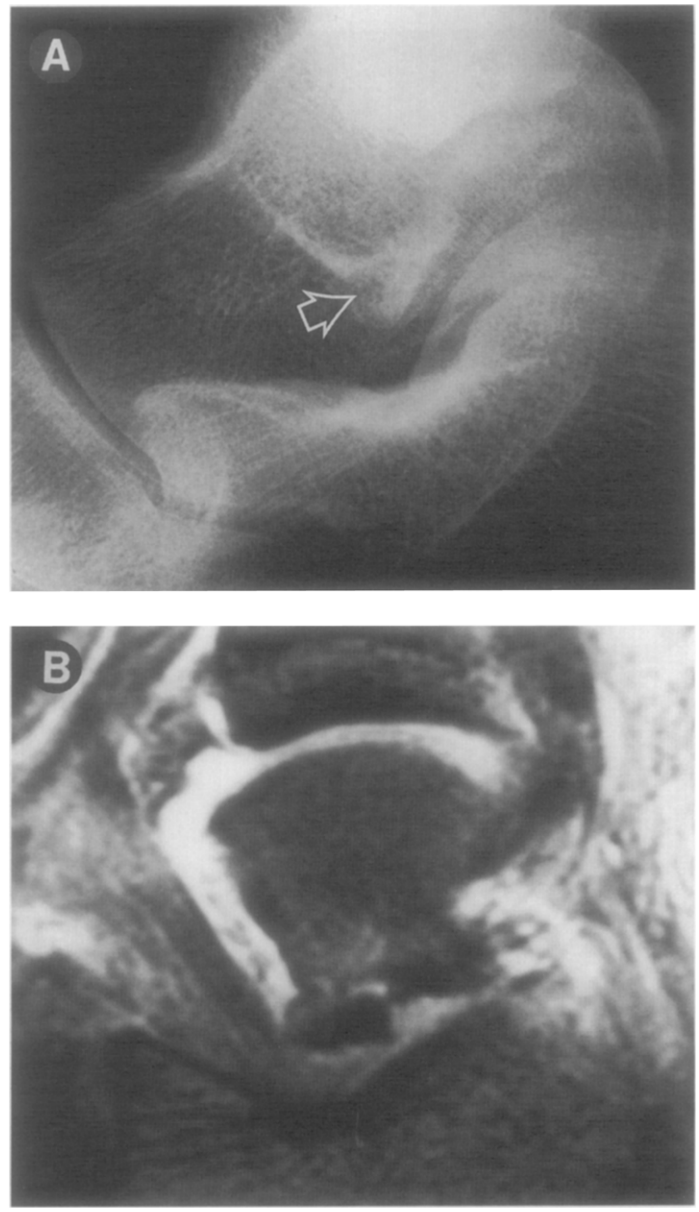

Fig 27. (A) Subtle lateral process fracture on lateral radiograph. (B) Gradient-echo images obtained to evaluate osteochondral lesion showed fracture through lateral process of talus.

Fig 29. (A) Normal frontal radiograph. (B) Coronal T1-weighted image shows transversely oriented fracture through distal tibial metaphysis (open arrow). (C) Normal lateral radiograph. (D) Sagittal T1-weighted image shows transversely oriented fracture line.

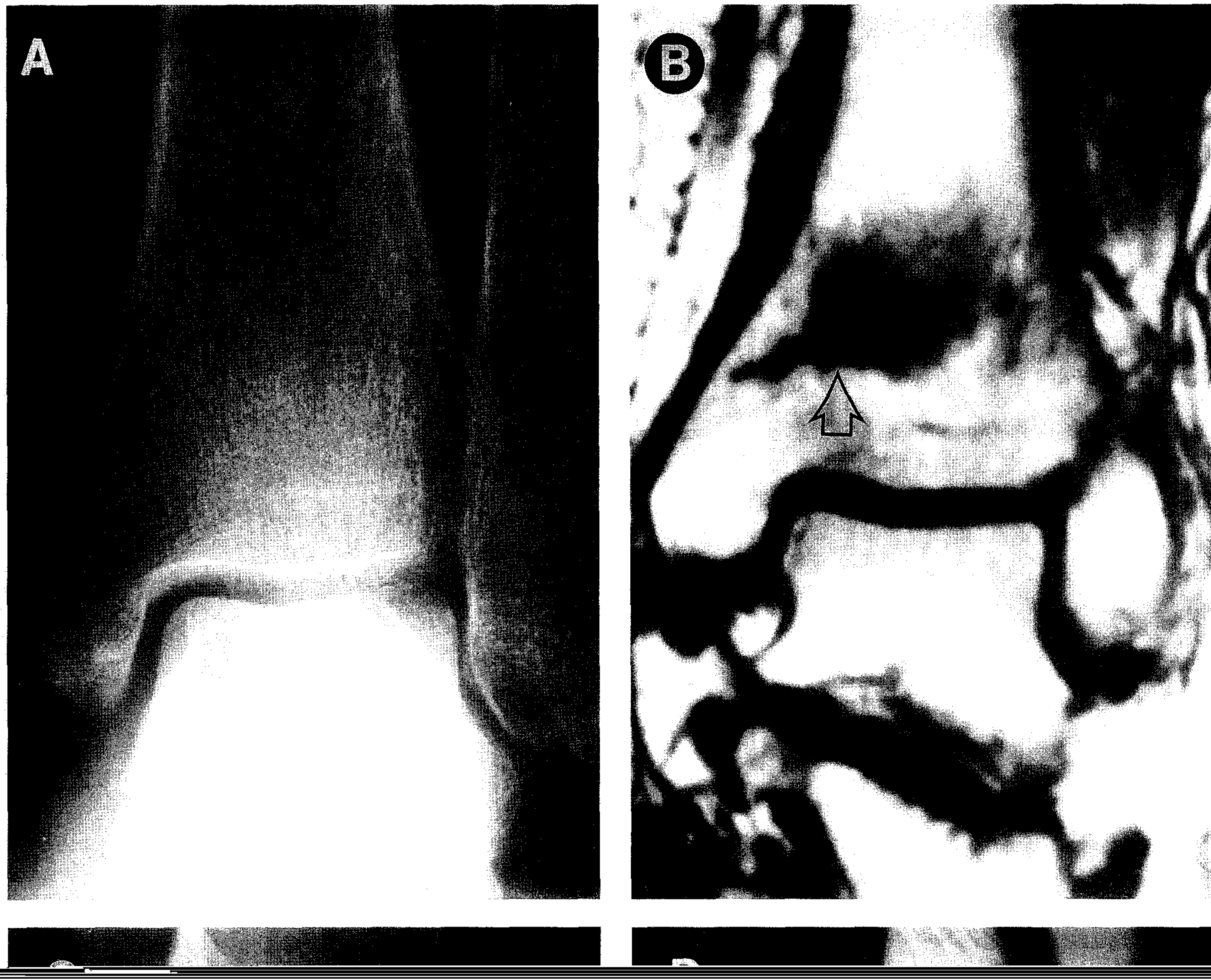
A
B